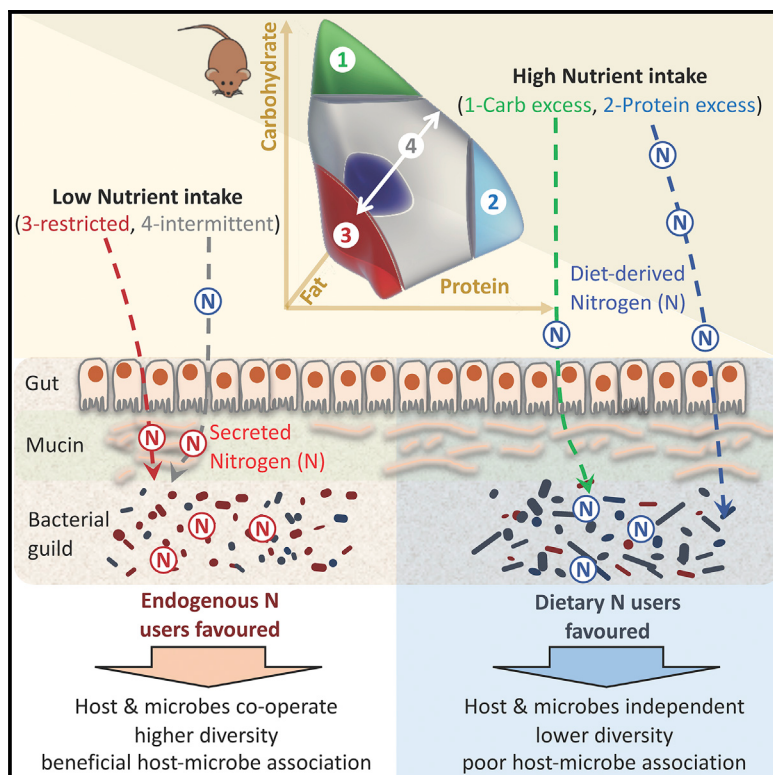


Cell Metabolism

Diet-Microbiome Interactions in Health Are Controlled by Intestinal Nitrogen Source Constraints

Graphical Abstract



Authors

Andrew J. Holmes, Yi Vee Chew,
Feyza Colakoglu, ...,
David Raubenheimer,
David G. Le Couteur,
Stephen J. Simpson

Correspondence

andrew.holmes@sydney.edu.au (A.J.H.),
stephen.simpson@sydney.edu.au
(S.J.S.)

In Brief

Diet interactively impacts the performance of animals and their microbes. Systematic analysis of intake across 25 defined diets in mice showed that microbial community assembly is fundamentally shaped by the relative amount of dietary nitrogen, providing a common factor for how different diets influence healthy host-microbiome outcomes.

Highlights

- Gut microbes show a dichotomy in ecological strategy for access to nitrogen
- Beneficial microbes are overrepresented in the endogenous N source guild
- Diets that reduce availability of dietary N to microbes promote healthy aging
- Diet impact on host-microbiome interaction can be simplified for modeling

Diet-Microbiome Interactions in Health Are Controlled by Intestinal Nitrogen Source Constraints

Andrew J. Holmes,^{1,2,7,*} Yi Vee Chew,² Feyza Colakoglu,² John B. Cliff,³ Eline Klaassens,^{1,2} Mark N. Read,^{1,2} Samantha M. Solon-Biet,^{1,2,4,5} Aisling C. McMahon,^{1,4,5} Victoria C. Cogger,^{1,4,5} Kari Ruohonen,⁶ David Raubenheimer,^{1,2} David G. Le Couteur,^{1,4,5} and Stephen J. Simpson^{1,2,*}

¹Charles Perkins Centre

²School of Life and Environmental Science
University of Sydney, NSW 2006, Australia

³The Centre for Microscopy, Characterization, and Analysis, University of Western Australia, Crawley, WA 6009, Australia

⁴Centre for Education and Research on Aging, and Aging and Alzheimers Institute, Concord Hospital, Sydney, NSW 2139, Australia

⁵ANZAC Research Institute, Sydney, NSW 2139, Australia

⁶EWOS Innovation, Dirdal 4335, Norway

⁷Lead Contact

*Correspondence: andrew.holmes@sydney.edu.au (A.J.H.), stephen.simpson@sydney.edu.au (S.J.S.)

<http://dx.doi.org/10.1016/j.cmet.2016.10.021>

SUMMARY

Diet influences health and patterns of disease in populations. How different diets do this and why outcomes of diets vary between individuals are complex and involve interaction with the gut microbiome. A major challenge for predicting health outcomes of the host-microbiome dynamic is reconciling the effects of different aspects of diet (food composition or intake rate) on the system. Here we show that microbial community assembly is fundamentally shaped by a dichotomy in bacterial strategies to access nitrogen in the gut environment. Consequently, the pattern of dietary protein intake constrains the host-microbiome dynamic in ways that are common to a very broad range of diet manipulation strategies. These insights offer a mechanism for the impact of high protein intake on metabolic health and form the basis for a general theory of the impact of different diet strategies on host-microbiome outcomes.

INTRODUCTION

How diet influences our health is a fundamental question for public health and individual interventions. Diet is the product of available foods and feeding behavior. Experimental manipulations of food composition or intake have repeatedly shown that changes in animal physiology are concomitant with changes in gut microbiome, and transplant experiments show that the diet-selected microbiome can have a causal contribution to these outcomes (David et al., 2014; Ridaura et al., 2013; Wu et al., 2015). However, the reproducibility of host outcomes in diet intervention studies is sensitive to food composition and genetic background of the animal model. Even more challenging is that

diet-selected microbiome composition is poorly reproducible between studies, and cross-sectional studies in humans seldom show clear associations between microbiome composition and host health. This implies the host-microbiome symbiosis is a metastable system capable of adopting different stable states. Consequently, predicting microbiome outcomes of diet manipulations, or defining the relative importance of diet and microbial contribution to host outcomes, is very difficult (David et al., 2014; Faith et al., 2013, 2014; Ridaura et al., 2013; Wu et al., 2015).

Predictive models require greater understanding of which dimensions of diet control emergent patterns of the gut ecosystem. It is well established that differences in microbial utilization of substrates in the diet have a significant impact on community composition (Sonnenburg et al., 2010). However, the effects of other aspects of diet composition on host animal biology further define the competitive environment for microbes in the intestinal tract. These diet-driven effects include behaviors such as appetite or food preferences (Lee et al., 2008; Simpson and Raubenheimer, 2005), and physiological responses such as gastrointestinal motility (Kashyap et al., 2013), intestinal secretions (Devkota et al., 2012), or inflammation (Lam et al., 2015; Stecher et al., 2007). Furthermore, microbial metabolism influences the host's sensing of the intestinal milieu and regulation of these responses (Cani et al., 2013). Such an abundance of interactions creates the potential for multiple feedbacks between available foods and host and gut microbiome that constrain emergent outcomes and will be important to understanding metabolism at the whole-organism level (Ley et al., 2006a; Wu et al., 2015).

A major challenge for modeling emergent diet-microbiome-host outcomes is that the microbiome is both species rich and has high levels of functional redundancy (Coyte et al., 2015; Donaldson et al., 2016; Faith et al., 2013). Thus, where the species (or OTU [operational taxonomic unit] surrogate) forms the unit of community description there is an almost infinite number of possible microbiome compositions that could contribute to a particular outcome for the host. In principle,

this issue can be reduced by different approaches to classification, whereby functionally similar species are lumped into higher taxa or communities are described in terms of gene composition. For example, association with obesity has been reported for the ratio of *Bacteroidetes* to *Firmicutes* (Ley et al., 2005, 2006b) or the metagenome gene count (Cotillard et al., 2013; Le Chatelier et al., 2013). These studies indicate there are systematic patterns to how diet drives microbial impact on health. However, this has not led to a general mechanistic explanation of the drivers of the microbial ecosystem or clear taxonomic or microbial gene signatures with predictive value for obesity outcomes (Finucane et al., 2014; Zhao, 2013). The reasons for this include (1) the low precision of higher taxon classification (the high levels of functional variation confounds between-sample comparisons), (2) limited ability to assign functions to genes in metagenomes, and (3) limited understanding of the interactive effects of environmental or genetic variation on system responses. Addressing questions oriented at emergent system properties requires a new conceptual and experimental framework for considering the nutritional determinants of the microbiome and the host response (Coyte et al., 2015). Here we show how systematic exploration of nutritional resource dimensions (Raubenheimer and Simpson, 2016) to describe bacterial community composition in terms of what resources they require (guilds) (Blondel, 2003) offers such a framework and identifies intestinal nitrogen as a fundamental driver of host-microbiome interactions in metabolism.

RESULTS

The Energy Density of Food Composition Has the Strongest Association with Change in Microbial Diversity

We systematically examined the impact of the compositional distribution and intake dimensions of diet on microbial community structure in the mouse. This was conducted in a framework that enables comparison with the physiological response of the animal. All diets were formulated from a fixed set of source components to minimize variation due to differences in palatability, digestibility, or bioactive properties of food components. The amounts of these components in each food were systematically varied to provide a total of 25 different diets encompassing ten macronutrient distributions and three different energy densities (Solon-Biet et al., 2014). Across the diet treatments, energy intake as protein (Prot) ranged from 5% to 60%, carbohydrate (Carb) from 20% to 75%, fat (Fat) from 20% to 75%, and energy density (E) from 2 to 4 kcal/g (8, 13, or 17 kJ/g). Animals were fed ad libitum. As a consequence of differences in diet energy density and compensatory feeding in response to Prot and Carb content, there was an approximately 2-fold range in energy intake across the study. Mean total caloric intake for the mice on the diets ranged from 24.98 to 54.03 kJ/day (Table S2; Supplemental Experimental Procedures, available online).

The data on microbial community composition are derived from pyrosequencing analysis of 16S rRNA amplicons from cecal metagenomic DNA samples of 112 C57BL/6 male and female mice that were culled at 15 months (out of a total of 858 animals). Technical replicates with independent DNA extraction from the same cecal samples were performed for ten mice.

Across the dataset, the average number of reads per sample after quality filtering was 12,000. Within each of the 25 diet treatment groups, the number of samples and reads ranged from 2 to 6 and 21,840 to 94,808, respectively (Figure 1A).

In human studies, collection of intake data is difficult and diet is commonly described qualitatively. Here, when the quality of the supplied food to the mice was considered with respect to the four diet composition variables, then the strongest effects on microbial diversity were observed for energy density. Analysis of alpha diversity across the diet treatments showed diversity was highest with low energy density, as shown for the inverse Simpson index (Figures 1B, S2A, and S2B). Diversity indices were sensitive to the weighting given to relative abundance, and taxonomic richness showed no significant differences at all examined scales (Figure 2). Community compositional relationships between the diet treatment groups (beta diversity) also showed a strong effect of diet energy density (Figures 1C and S2C–S2F). Fitting environmental gradients to CA (correspondence analysis) ordinations at different taxonomic scales (both genus and family) showed the explanatory power was greatest for dietary energy density (62.4%) and, to a lesser extent, Fat and Carb content (Figure S3). This is consistent with the enormous volume of studies showing diets with high Fat content or high caloric intake are obesogenic and drive strong microbial changes. In summary, if we simplify diet characterization to the quality of supplied food in terms of its caloric density and macronutrient distribution, then long-term effects of diet composition on the gut microbiota are primarily related to food energy density and reflect shifts in abundance distribution more strongly than taxonomic richness. The significance for the animal is thus predicted to lie in change in relative strength of microbial signals, rather than gain or loss of microbial properties.

The Intake Rate of Prot and Carb Is the Major Driver of Microbial Response

These associations to diet composition do not indicate that Fat or total calories per se are important mechanistic drivers of microbial response. Animals regulate their food selections and intake according to nutritional quality. Furthermore, not all food components are equally accessible to the cecal or colonic microbiota. To parse the effects of diet composition into macronutrient intakes, we next looked at abundance changes of major microbial taxa in response to daily energy intakes of Prot, Carb, and Fat, considering both their main and interactive effects. Generalized additive models (GAMs) and thin-plate splines were used to analyze and visualize the community response to Prot, Carb, and Fat intakes using measures of diversity and relative abundance of major bacterial taxa. Surprisingly, the models indicated that for all measures of community response, the major drivers of change were Prot and Carb intake, while Fat intake had a very minor role (Figures 3 and S4; Table S1). In the case of total community measures, the inverse Simpson index decreased with increased intake of Prot and Carb (Figures S2A and S2B). In the case of taxon response, Prot and Carb intake were again the major drivers, but two basic taxon response patterns were seen (Figures 3 and S4; Table S1): an increase or a decrease in relative abundance with Prot and with Carb intake. We termed this a consumption-type response or limitation-type response,

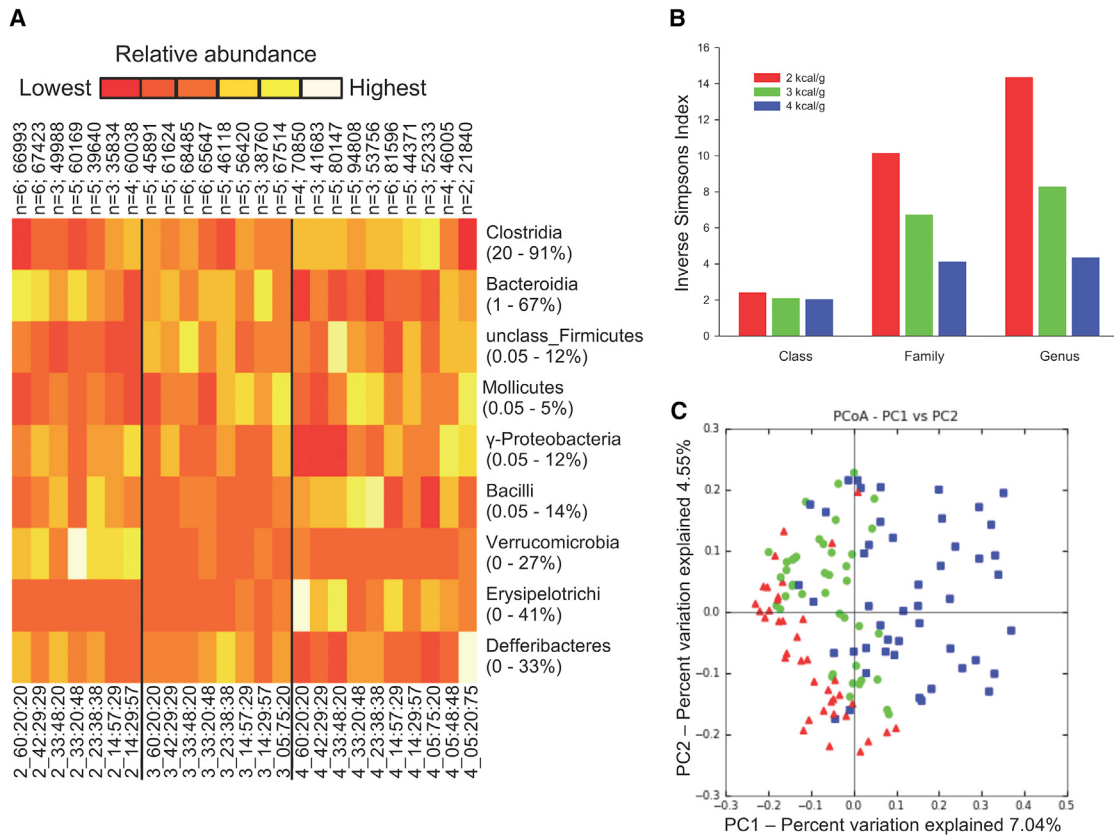


Figure 1. The Energy Density of Diet Compositions Exerts Strong Effects on Microbial Diversity

(A) Microbial cecal community dataset viewed as a heatmap of rank abundance at the higher taxon level. A total of 112 mice were maintained on 25 different diet formulations varying in macronutrient distribution and density. Top text strip shows pooled number of sequence reads and number of individual mice for each diet formulation. Bottom text strip shows diet formulations clustered in groups of similar energy density (e.g., Diet 2_60:20:20 is 2 kcal/g density with macronutrient distribution of 60% Prot, 20% Carb, and 20% Fat). Side text strip shows the range of relative abundances for indicated taxonomic groups.

(B) Effect of diet energy density on microbial diversity defined by the inverse Simpson diversity index at three taxonomic scales (all samples of same energy density were pooled).

(C) Principal coordinates analysis plot of unweighted UniFrac distances by diet energy density treatment groups.

See also Figures S1 and S2.

respectively. There was a strong concordance between the direction of changes in various aspects of host phenotype (e.g., body weight, body composition, and metabolic parameters) and whether the various OTUs belonged to either the guild that demonstrated a limitation-type response or the consumption-type response (Table 1).

We next considered the reproducibility of phylogeny-based classification as a metric for description of ecological patterns across animal populations. Examples of response surfaces for higher taxa that have a high relative abundance signal across the dataset are shown in Figure 3 (Figures 3 and S4; Table S1). For the *Verrucomicrobia* and *Erysipelotrichia*, each is predominantly comprised of OTUs assigned to one genus (*Akkermansia* and *Allobaculum*, respectively) and response surfaces at class and genus scale are essentially the same. Consequently, across all samples in the dataset the relative abundance of these higher taxa is predicted be the result of a similar ecological response. In contrast, the two most abundant taxa in our dataset, the *Bacteroidetes* and *Firmicutes*, encompass very large numbers of OTUs representing a wide spectrum of phylogenetic

distances and large number of genera. Although both had surfaces with high explanatory power (Table S1), the subtaxa of these phyla showed distinct responses. This was most obvious with the *Firmicutes* subtaxa, where *Ruminococcaceae* and *Lachnospiraceae* showed limitation-type responses and *Clostridiaceae* and *Erysipelotrichaceae* showed consumption-type responses (Figure S4; Table S1). A consequence of this is that in the gut community of animals with differing levels of Prot and Carb intake, the competitive advantage for species within the phylum *Firmicutes* also differs. It follows that in any one gut microbiome, the net change in *Firmicutes* abundance in response to diet will be highly dependent on the starting species composition. Consequently, phylogenetically defined higher taxa such as the *Firmicutes* and *Bacteroidetes* lack the biological precision needed for effective modeling of diet responses across natural animal populations where genetic and environmental heterogeneity underpin high variation in species composition. For modeling purposes, there is a need to define higher taxa whose response to ecological mechanisms will be consistent across all populations.

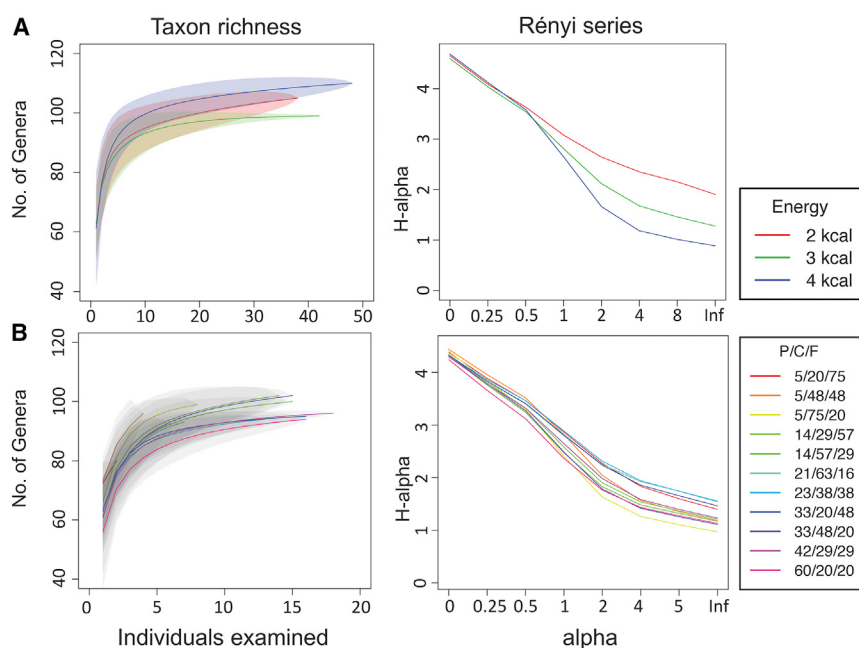


Figure 2. Accumulation Curves and Renyi Plots

(A) Accumulation curves (left panel) and Renyi diversity profiles (right panel) for genus-level data pooled by diet energy density (32–40 mice per group). At this taxonomic scale, curves are approaching saturation after five individuals (approximately 50,000 reads). Shading indicates 95% confidence limits. Differences in diversity are only seen when the weighting abundance (α) becomes greater than 1 (corresponds to Shannon index).

(B) Accumulation curves (left panel) and Renyi diversity profiles (right panel) for genus-level data pooled by their macronutrient composition as %P/%C/%F (2–16 per group). Differences in diversity are only seen when comparing across the extremes of macronutrient distribution.

next considered what mechanisms might underpin the distinction between the two major trophic response guilds with respect to Prot and Carb intakes. Those taxa that show higher relative abundance

in low Prot and Carb intake regions of nutrient intake (e.g., *Bacteroidetes*, *Verrucomicrobia*, *Lachnospiraceae*, and *Ruminococcaceae*) include many species with the ability to utilize host proteoglycans such as mucin (Berry et al., 2013; Derrien et al., 2008; Macfarlane et al., 2005). On the basis of model simulations, we postulated that the mechanism by which nutrient intake may drive community change is alteration of the relative importance of dietary nutrients with endogenous host secretions as a source of carbon and/or nitrogen to bacteria (Figure S5). Importantly, this would provide a mechanism to explain microbiome response across dimensions of dietary composition (nutrient profile) and intake pattern (both integrated total intake or temporal pattern). Such a model is necessary to reconcile microbial impact across diet strategies that manipulate intake such as caloric restriction and time-restricted feeding or fasting with those that emphasize composition such as healthy Fat or Carb profiles.

Host Processes Control Microbiome Dynamics through Regulation of Intestinal Nitrogen Availability to Bacteria

To test the generality of this hypothesis and further explore the mechanism, a second experiment was performed in BALB/c mice. Intake of Prot and Carb was manipulated by feeding mice diets of comparable macronutrient distribution, but different energy density. After 3 weeks on the diets, $^{13}\text{C}^{15}\text{N}$ -threonine was injected into the tail vein (threonine is a major component of mucin). After 24 hr, samples were taken for microbial community analysis by pyrosequencing and determination of bacterial uptake of carbon and nitrogen by nanoSIMS.

The diet-induced changes in total *Bacteroidetes* and *Firmicutes* abundance across the two energy densities were consistent with the previously observed limitation and consumption responses, respectively. Total abundance of *Bacteroidetes* was higher in the 2 kcal/g diet and total abundance of *Firmicutes* was higher in the 4 kcal/g diet (Figure S5C). Furthermore, there

Simple Mechanisms Underpin the Impact of Nutrient Intake on Host-Microbiome Dynamics

In our dataset, although the relative abundance distribution across nutrient intake space differed widely across bacterial taxa, we only observed two main response patterns: increase, or decrease in relative abundance with Prot and Carb intake. Fat intake had little effect, either alone or in interaction. Notably, in the case of *Firmicutes*, the parent taxon showed positive response to Prot and Carb intake with few interactive effects, despite several significant subtaxa showing the opposite response. The lack of consistent response within phylogenetically defined groups shows that higher taxa defined in this way lack the biological precision necessary for predictive models. However, the strong recurrence of the same two response patterns at all scales indicates a fundamental distinction in life history strategy for gut bacteria that is based around the host's dietary Prot and Carb intake. This conclusion is consistent with our observations on diversity. Diversity was more strongly shaped by changes in relative abundance than species composition (Figure 2). The response surface for the inverse Simpson index showed the major drivers of this were Prot and Carb intake (Figures 1B, S2A, and S2B). Finally, there is a wider range of genera that increase in abundance with lower Prot and Carb intake (Figure S4; Table S1). On this basis, we propose that dietary impacts on host-microbiome dynamics are underpinned by far simpler ecological mechanisms than anticipated. The significance of this is that the host can exert regulatory control on the microbial contribution to its immune-metabolic functions through feeding behavior.

A prediction of this model is that the dominant processes of microbial community assembly and microbiome relationship to emergent properties of the host will be more effectively captured by exploiting the concept of trophic response guilds—sets of taxa that show common response patterns to resource availability—than by phylogenetic relationships (Blondel, 2003). Thus, we

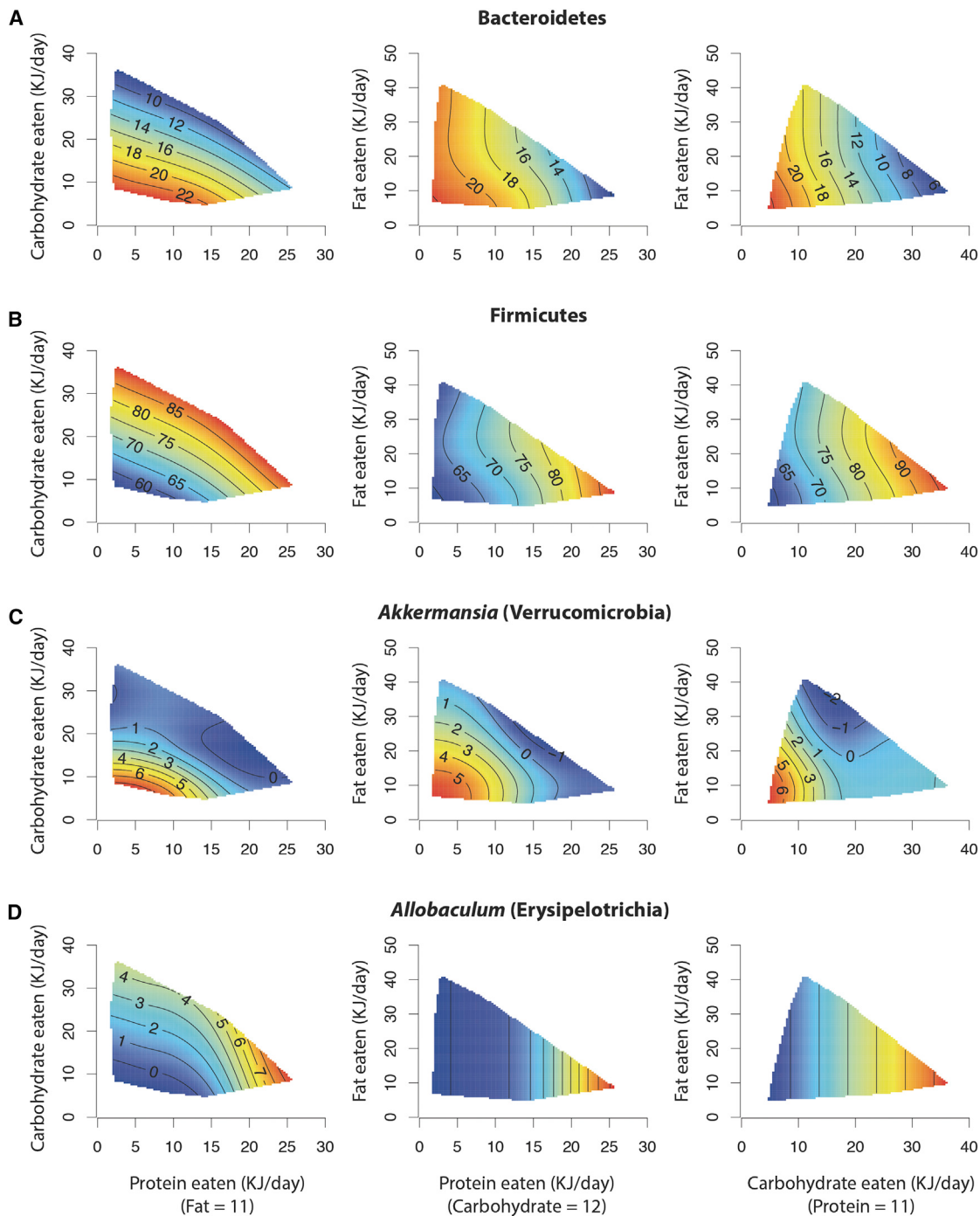


Figure 3. Macronutrient Intake Drives Two Main Responses in Relative Abundance of Major Taxa

Major phyla are (A) Bacteroidetes and (B) Firmicutes. Example genera are (C) *Akkermansia* (Verrucomicrobia) and (D) *Allobaculum* (Erysipelotrichia). Three slices of nutrient intake space are shown to visualize all three dimensions. Prot, Carb, and Fat intake are shown as kJ/day. The two-dimensional surface for each combination of two macronutrients is shown at the median of the third macronutrient (indicated on x axis). Red, highest abundance; blue, lowest abundance. See also Figure S3.

were some differences in the dominant subtaxa seen in this study, and again we observed some divergence in responses by genera within the higher taxa. In these BALB/c animals, the *Bacteroidetes* class was dominated by OTUs assigned to *Bacteroides*, *Barnesiella*, and *Parabacteroides*, and *Firmicutes*

were dominated by *Bacilli*, rather than *Clostridia*. Within the *Bacteroidetes*, a limitation-type response was observed for *Bacteroides* and *Parabacteroides*, but *Barnesiella* showed the opposite strategy with significantly higher relative abundance in the 4 kcal/g diet treatment.

Table 1. Correlation between Gut Microbiota Classified According to “Limitation-type Response” versus “Consumption-type Response” versus Host Phenotype and Circulating Amino Acids

| Mouse Phenotype | Microbiome | Body Weight | Percent Fat | Fat Mass | Lean Mass | BMD | Glucose | Cholesterol | HDLc | Leptin |
|----------------------------------|------------|-------------|-------------|-----------|-----------|------------|---------|-------------|------|---------|
| Limitation-type Response | | | | | | | | | | |
| Bacteroidetes | ** | — | * | ** | ** | ** | ** | ** | ** | * |
| Deferribacteres | — | — | — | * | * | — | — | — | — | — |
| Verrucomicrobia | * | ** | ** | * | ** | ** | — | — | — | ** |
| Lachnospiraceae | — | — | — | — | ** | — | — | — | — | — |
| Ruminococcaceae | * | ** | * | — | ** | — | — | — | — | — |
| Eubacteriaceae | — | * | — | — | ** | * | — | — | — | — |
| Rikenellaceae | ** | — | * | ** | ** | * | * | ** | — | — |
| Bacteroidaceae | * | — | — | * | ** | — | * | * | * | — |
| Consumption-type Response | | | | | | | | | | |
| Firmicutes | ## | # | ## | ## | ## | ## | ## | # | # | ## |
| Clostridia | ## | — | # | ## | ## | # | # | # | # | # |
| Clostridiaceae | ## | ## | ## | ## | ## | ## | ## | — | # | ## |
| Erysipelotrichia | — | — | — | — | ## | — | — | — | — | # |
| Circulating Amino Acids | | | | | | | | | | |
| Microbiome | | Citrulline | | Ornithine | | Tryptophan | | Tyrosine | | Glycine |
| Limitation-type Response | | | | | | | | | | |
| Bacteroidetes | ## | — | | ## | | ## | | — | | — |
| Deferribacteres | — | — | | — | | — | | — | | — |
| Verrucomicrobia | ## | ## | | — | | — | | — | | — |
| Lachnospiraceae | # | # | | — | | — | | — | | — |
| Ruminococcaceae | — | — | | — | | — | | — | | # |
| Eubacteriaceae | — | # | | — | | — | | — | | — |
| Rikenellaceae | # | # | | — | | — | | # | | — |
| Bacteroidaceae | ## | # | | ## | | ## | | # | | — |
| Consumption-type Response | | | | | | | | | | |
| Firmicutes | ** | * | | * | | * | | * | | — |
| Clostridia | ** | — | | * | | * | | * | | — |
| Clostridiaceae | ** | ** | | — | | — | | — | | * |
| Erysipelotrichia | ** | * | | — | | — | | — | | * |

Correlations determined by Pearson’s correlation coefficient: *p < 0.05 and **p < 0.01 for negative correlation, and #p < 0.05 and ##p < 0.01 for positive correlation. Across this analysis, only outcomes where more than three taxa are significantly correlated are shown; bacillae could not be classified as either limitation- or consumption-type response. BMD, bone mineral density; HDLc, high-density lipoprotein cholesterol. See also [Table S1](#).

Significant differences in the bacterial uptake of label between the two diet treatments were observed in the nanoSIMS analysis. For both ¹³C and ¹²C-¹⁵N detection, a high proportion of total cells in the 2 kcal/g treatment were labeled more strongly than any cell from the background control treatments ([Figure 4](#)). For ¹²C-¹⁵N, there was also higher labeling in the 4 kcal/g treatment relative to background controls. Also, the ¹²C-¹⁵N signal must reflect cleavage of the ¹³C-¹⁵N bond in the labeled threonine and reformation of a CN bond. In conjunction with the different distributions for these two ions across the diet treatments, this almost certainly reflects different levels of bacterial use of the threonine-derived nitrogen in biosynthetic pathways rather than abiotic formation of the ¹²C-¹⁵N ion during imaging. The extent of labeling of cells was not normally distributed ([Figure S5B](#)), and morphometric analysis revealed a strong correlation between cell width and labeling: thin cells were more strongly

labeled under both diet treatments. Importantly, for gut microbes in the low energy density diet treatment, both the labeling intensity and the relative abundance of the thin morphotype cells increased with respect to the thick morphotype ([Figure 4](#)). This supports our interpretation that increased utilization of endogenous nutrient sources (especially nitrogen) provides selective advantage under low nutrient intake conditions. Although it is not possible to identify these cells, we note that the sequence data predict the major shift in the gut community was due to a shift in the relative dominance of *Parabacteroides* (higher in 2 kcal/g diet) and *Barnesiella* (higher in 4 kcal/g diet), and thin and thick cell morphology, respectively, is consistent with these two genera.

To further test the extent to which ecosystem-level control on community assembly could occur via nitrogen competition, we developed an agent-based simulation ([Figures 5, 6, and S6](#)).

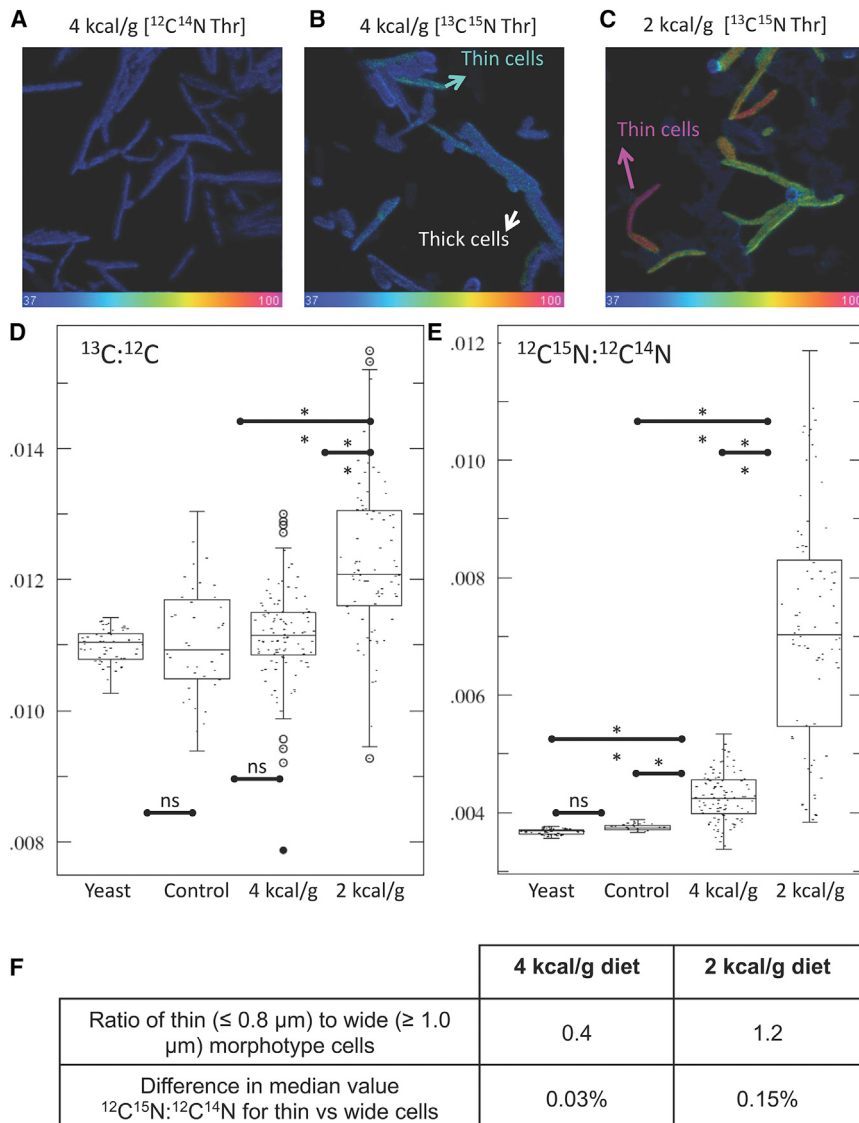


Figure 4. Bacterial Uptake of Intestinal Secretions under Different Diets Determined by nanoSIMS

(A–C) Images of $^{12}\text{C}^{15}\text{N}$ ion distribution in colon microbes.

(A) Untreated control: mouse maintained on 4_21:63:16 diet with no labeled threonine injection.

(B) Mouse on 4_21:63:16 diet before intravenous injection of $^{13}\text{C}^{15}\text{N}$ -threonine.

(C) Mouse on 2_14:57:29 diet before intravenous injection of $^{13}\text{C}^{15}\text{N}$ -threonine.

(D and E) Box and whiskers plots showing isotope ratio per cell for indicated mass species. The plot indicates the median (horizontal line in box), the middle 50% of values (box), and the minimum and maximum values.

(F) Change in morphotype relative abundance under diet regimes corresponds to the extent of utilization of ^{15}N . * $p < 0.05$; ** $p < 0.01$.

See also Figure S4.

Our modeling approach is based on partitioning the community into six guilds whose cell replication rate is based on acquisition of carbon and nitrogen from different dietary and endogenous sources. Death rate is based on starvation or loss through defecation. In each simulation, the community self-assembles from a small starting population of all six guilds as the animal is “fed” a diet of defined macronutrient composition according to typical day/night feeding patterns of mice. The carrying capacity of the simulated gut and relative abundance of each guild stabilized over 3–5 days of simulated time and are products of their competition for carbon and nitrogen from the dietary and endogenous sources. Repeating simulations across a range of macronutrient intakes generated datasets for construction of response surfaces. The simulation outputs for guild abundance are based on the known intakes of 250 mice from this study. These show that tension between dietary and endogenous sources of nitrogen can drive shifts in global community composition. The extent of this simulated community response is comparable to the exper-

imentally observed shifts in higher taxa. Of particular importance is that in the region of intake space observed to be associated with cardiometabolic health (low Prot and high Carb intake), the simulation predicts nitrogen to be a limiting nutrient for four of the six guilds, and in the region of intake space where cardiometabolic health is poorest, the simulation predicts nitrogen limitation is lost (Figure 5). Finally, for a number of genera, including *Parabacteroides*, GAMs constructed from the experimental data show close correspondence to the guilds predicted by their physiology. This supports our hypothesis that host manipulation of intestinal nitrogen availability has a key role in regulation of the host-microbiome dynamic.

Intestinal inflammation is widely thought to act as a key driver of microbial dysbiosis through a positive feedback loop involving poor microbial support of intestinal epithelial functions, increased permeability of the gut epithelium, poor host regulation of the inflammatory response, and an increase in inflammatory microbial signals (Lam et al., 2015). To evaluate the relationship between intestinal function and microbiome, we measured circulating citrulline, which is an amino acid produced only by enterocytes and proposed as a biomarker of intestinal function (Peters et al., 2011; Breuillard et al., 2015). There was a positive correlation between citrulline and the abundance of OTUs that have a limitation-type response and a negative correlation between citrulline and the abundance of OTUs that have a consumption-type response (Table 1). This is consistent with the concept that low Prot diets are associated with increased intestinal function leading to an increase in available host-generated nitrogen to sustain microbiota with a limitation-type response to diet. We have previously shown that mice on low Prot, high Carb diets have larger intestines, caeca, and colons (Sørensen et al., 2010).

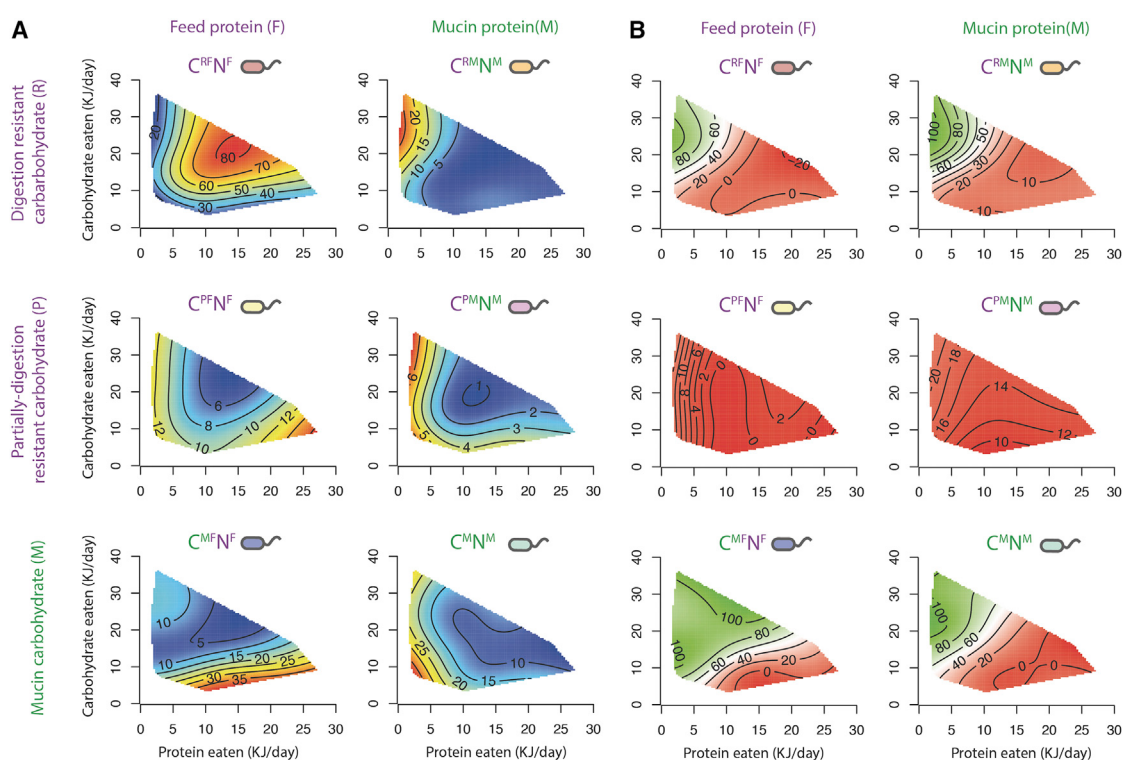


Figure 5. Simulated Microbiota Responses to Nutrient Intake and Mucin Abundance

(A) Trophic guilds comprising a simulated microbiota show distinct relative abundance responses to changing nutritional intake. Relative abundance response landscapes within a nutritional intake space are shown as a matrix, with columns and rows describing each guild's Prot and Carb substrates, respectively. Relative abundances arising from each nutritional intake are determined at 3 weeks of simulated time. Landscapes are generated by fitting a generalized additive model to 250 simulations; method is as described for the bacterial taxon abundance landscapes.

(B) Carbon or nitrogen limitation experienced by individual cells is predicted to vary with nutrient intake, trophic strategy, and competitive environment. In the simulation, cell status is simulated by acquired carbon and nitrogen resources. The response surface models the proportion of cells (%) comprising each guild that are nitrogen limited. Limitation is a function of both supply and competition with other guilds. Regions where the dominant limiting factor is nitrogen (values above 50%) are shaded green and regions where the dominant limiting nutrient is carbon are shaded red (values below 50%).

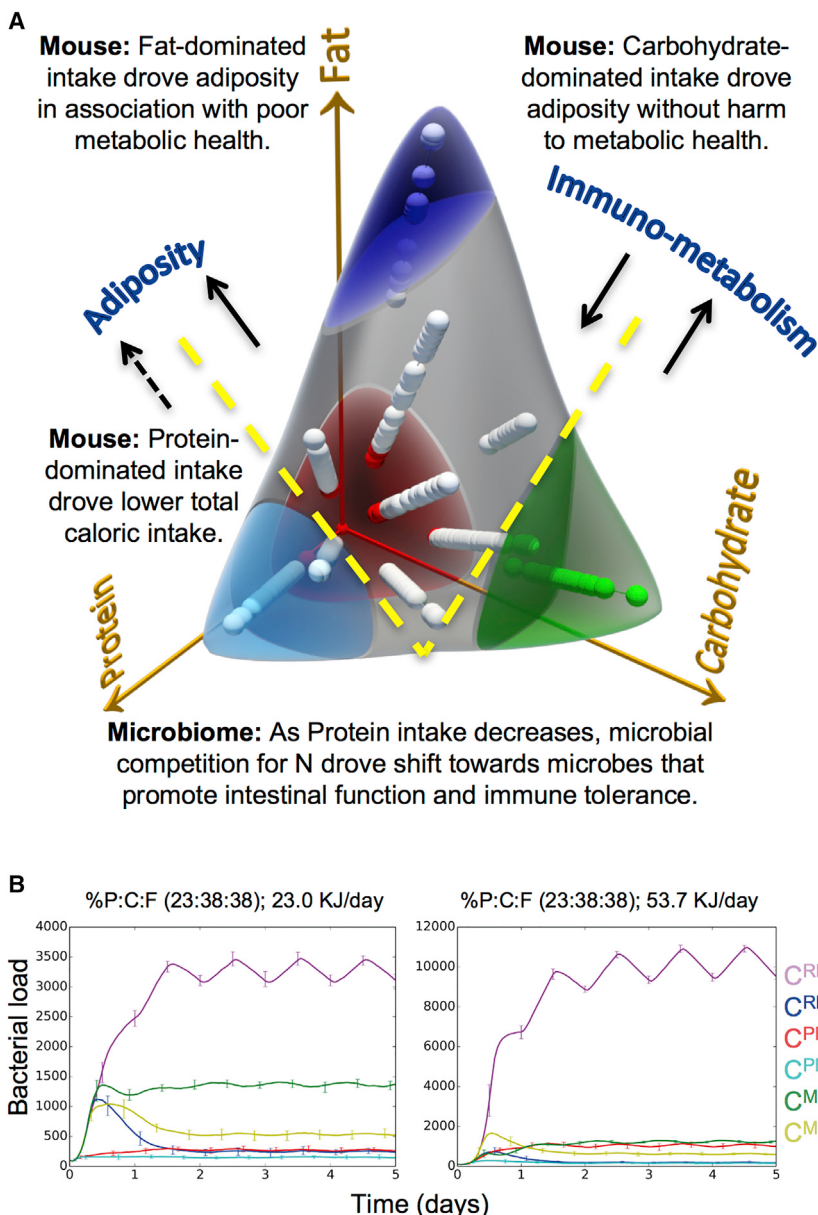
DISCUSSION

The health of an animal is dependent upon its ability to regulate metabolism across a range of spatiotemporal scales. The availability of food and the activity of gut microorganisms are two factors that profoundly influence systemic metabolism, but are not under the direct control of animal systems. Given the natural variability of access to food for all animals, we postulate that evolution of stable host-microbiome associations will have been broadly shaped by the host ability to integrate feeding behavior and microbiome performance with its immune and metabolic functions. This is consistent with the view that in many modern lifestyle diseases, the roles of diet and the gut microbiome are linked. Here we show that the major diet impact on the gut microbial ecosystem can be simplified to combined Prot and Carb intake and that the alignment of Prot and Carb intake with healthy aging is consistent with a critical role for nutritional regulation of microbiome health via intestinal nitrogen availability.

Our model predicts that at the community level, microbial use of Carb resources will be tightly coupled to nitrogen availability across disparate Carb profiles. Thus, while Carb profile shapes microbial diversity through individual species substrate prefer-

ences (Koropatkin et al., 2012), dietary Prot levels and periodicity of total caloric intake will consistently shape the outcomes of competition for Carb substrates. The host ability to manipulate Prot and Carb intake patterns has thus shaped the evolution of the beneficial relationship with its microbiome. A consequence of this resource-based regulation is that the guild concept, classification by resource access (as opposed to functional properties), is an effective way to mechanistically model the primary effect of diet on gut ecosystem functions, and that substrate preferences can be viewed as a secondary layer of diet response (albeit one giving strong signals). The response surfaces provide an integrative framework for associating change in the microbial ecosystem with host physiology and emergent health.

Comparing microbial and physiological outcomes in the four extreme regions of macronutrient intake space indicates connections between intake patterns, microbial resource use, and known mechanisms of microbial influence on health. There is an emerging consensus that intestinal permeability, mesenteric fat, and inflammation are key drivers of metabolic health outcomes (Cani et al., 2013; Lam et al., 2015; Wu et al., 2015). Here, adiposity and immuno-metabolic health responded differently to dietary macronutrient balance, and poor health



resulted where these drivers intersected (Solon-Biet et al., 2014). Adiposity was primarily driven by total caloric intake (increased in all three dimensions) but was exacerbated on diet compositions with low Prot that promote compensatory feeding. However, the association of health with adiposity was influenced by macronutrient distribution. Health was highest when caloric intake was dominated by Carb; poor cardio-metabolic parameters and shortened lifespan resulted when Prot or Fat dominated intake. Mice in the region of highest Prot intake showed the attributes of immunosenescence (Claesson et al., 2012), and Prot intake far more strongly affected relative levels of CD4 and CD8 lymphocytes than any other macronutrient, suggesting high Prot diets will pre-dispose to altered immuno-regulatory states (Le Couteur et al., 2015).

Reconciling these outcomes with the microbiome responses gives a model for diet-host-microbiome interaction where

Figure 6. A Nutritional Ecology View of the Host-Microbiome Dynamic and Major Tipping Points Influenced by Intestinal Nitrogen Availability

(A) Each ball inside the space is the observed nutrient intake of a mouse in this study in terms of Prot, Carb, and Fat. The outward-facing surface shows the three extremes of macronutrient distributions that can occur under high caloric intake diets, and the red-colored rear surface represents the lower extreme of caloric intake. A fundamental ecological constraint on microbial access to dietary Carb that passes beyond the small intestine is competition for nitrogen. There is a dichotomy in microbial strategies to meet this constraint whereby either dietary or host nitrogen sources are exploited. Mouse phenotypes with improved metabolic health are associated with microbiomes dominated by host-N strategy microbes and can be shifted by the ratio of microbially accessible Carb to nitrogen in the food (or during periods of fasting).

(B) Effect of restricted caloric intake on bacterial load over time in simulated mice gut communities. The average of 50 independent simulations of mice with two different intake rates of a chow with the same macronutrient distribution is shown. The simulations start with 100 cells of each guild at the commencement of the night-active phase. The emergence of stable community composition within 2 days and diet periodicity in bacterial load seen here was typical for all simulated nutrient intakes.

See also Figure S6.

intake of Carb is associated with support of microbial interactions that are beneficial by reducing age-related inflammation (Sonnenburg and Sonnenburg, 2014), but that the relative amount of dietary Prot determines the extent to which benefits to the host are realized. In this model, a high-Fat diet deleteriously impacts the host-microbiome dynamic through dilution of Prot and Carb

intake to the extent that it is insufficient to meet host (Prot) or microbiome (Carb) nutritional demands. This is consistent with the non-viability of the low-density versions of diets on this axis and very weak microbial response to Fat intake. The deleterious impact of Prot in our model is via change in the nature of microbes responding to Carb intake. Taxa with limitation-type response surfaces include species known to contribute to maintenance of intestinal barrier functions and immunoregulation, through butyrate production (Donohoe et al., 2011) and maturation of regulatory T cells (Atarashi et al., 2011; Mazmanian et al., 2008).

Our model also provides a mechanism to explain the range of microbiome and host outcomes in diet-induced obesity that is consistent with published observations on the change in ratio of *Bacteroidetes* and *Firmicutes* (Ley et al., 2006b) and gene counts (Le Chatelier et al., 2013). With the food components

used here, we found that consumption-type responses to diet were overrepresented in the *Firmicutes*. This pattern predicts *Firmicutes* abundance has a positive association with increased caloric intake and negative association with caloric restriction across a wide range of diets. Thus, although the ratio of *Bacteroidetes* to *Firmicutes* abundance varies widely between individuals (Finucane et al., 2014; Wu et al., 2011) and has limited value as a predictor of health status, the change in this ratio is likely to reflect diet impact on weight change. Although we did not measure gene counts, diversity is a strong predictor of gene richness and was shown here to be higher under diet regimes that select for limitation-type responses. Moreover, those species that were observed to be overrepresented in the HGC (high gene count) microbiomes (e.g., *F. prausnitzii*) (Le Chatelier et al., 2013) belong to taxa that we observed to have a limitation-type response.

In conclusion, our data indicate a key role for relative availability of intestinal nitrogen sources in diet outcomes and predict mechanisms through which host-microbiome relationships can be shifted (Figure 6). Recognition of the mechanistic roles of both dietary macronutrient profile and intake rate leads to opportunities to greatly simplify how we conceptualize the complex diet-host-microbiome dynamic for the purposes of modeling. In the *Supplemental Information*, we present an agent-based model for community assembly based on this general theory for diet control. Systematic simulations of assembly of hundreds of microbial communities on different diet regimes resulted in a spectrum of stable community compositions comparable to that seen for our experimental diet manipulations (Figure S5). Significantly, the topologies of simulated response surfaces were very similar to observed taxa and predict that nitrogen limitation is a feature of the bacterial community in regions associated with health. Thus, our experimental data and models show that nitrogen source constraints on microbial competition for Carb substrates exert sufficient control on community assembly to shape host-microbiome interaction. This mechanism is predicted to influence microbiome outcomes across a broad range of diet interventions, including intake-based strategies, such as caloric restriction or intermittent fasting (Mattson et al., 2014), and composition-based strategies, such as high Prot, high fiber, or prebiotic supplementation. We also predict that it would play a role in pathology of diseases such as gout associated with altered rates of excretion of nitrogenous waste through the intestine. The challenges for diet interventions now are to relate the microbiome impact more directly to health outcomes and to begin to explore the interactive contributions of different Carb, Prot, or Fat profiles with intake patterns. This requires highly multi-factorial experiments whose design will be facilitated by the agent-based model strategy developed here.

EXPERIMENTAL PROCEDURES

Long-Term Nutrient Intake Experiment

A total of 858 mice (strain C57BL/6) were maintained on 25 diets of defined composition and phenotyped at 15 months as described (Solon-Biet et al., 2014) (*Supplemental Experimental Procedures*). All protocols were approved by the Sydney Local Health District Animal Welfare Committee (Protocol No. 2009/003).

Microbiome Analysis

A subset of animals were euthanized and dissected at ~15 months for detailed analysis of physiology and microbiota (n = 112; 2–6 animals per diet treatment; Table S1). An additional five animals maintained on standard chow (AIN3G: Specialty Feeds) were also analyzed. All individuals selected for this analysis were from separate cages and samples were collected between 10:00 a.m. and 12:00 p.m. to minimize possible circadian effects. The entire intestinal tract was removed and cecum contents were collected aseptically by pipette. Total metagenomic DNA was recovered using the FastPrep DNA extraction kit and the microbial community sampled by 454 sequencing of the 3' end of the 16S ribosomal RNA (907–1492) using primers specific for the domain bacteria (Lam et al., 2012). After quality filtering, the average number of reads per sample was over 12,660. Sequence reads were assigned to OTUs at 97% identity and then classified using QIIME (Caporaso et al., 2010) or Mothur (Schloss et al., 2009). Unless otherwise stated, figures represent analyses based on the QIIME analysis using the RDP classification. The dataset is summarized in the *Supplemental Experimental Procedures* and was broadly typical of mammalian gut microbiota with samples dominated by members of a limited number of bacterial phyla (Donaldson et al., 2016; Ley et al., 2006a).

Isotope Tracer Experiment

To assess the utilization of host-derived nutrients by gut bacteria on diets of different energy density, eight female wild-type BALB/c mice (*Mus musculus*) were placed on defined diets (two or three per cage). Three animals were transitioned to the low energy density diet (2 kcal/g and 14:57:29 P:C:F ratio) over a period of 1 week, then maintained solely on that diet for a further 2 weeks. The remaining animals were housed in a cage of two or three animals and fed high energy density standard chow (4 kcal/g, 21:63:16 P:C:F ratio) for 3 weeks. Custom diets were obtained from Specialty Feeds.

After 3 weeks, both cages of three mice were injected intravenously into the tail vein with 2.1 μ mol/g body weight L-threonine containing 98% ^{15}N and 98% ^{13}C (CortecNet). The remaining two high energy density-fed mice were non-injected controls. The mice were monitored over the next 36 hr, with fecal samples collected at 6 hr intervals. At 24 hr post-injection, two mice from each diet set trio were culled and ascending colon contents were collected. All samples were frozen at -20°C immediately following collection.

A total of 5 mg of each colon sample was homogenized and washed in 1 x PBS buffer before cells were fixed in 4% paraformaldehyde. Fixed cells were resuspended in 50% (v/v) ethanol:PBS and stored at -20°C until analysis. Imaging work was conducted at the Australian Microscopy and Microanalysis Research Facility (AMMRF) at the University of Western Australia using the Cameca NanoSIMS 50 (Cameca) or scanning electron microscopy using Zeiss 1555 VP-FESEM. A total of 10 μL fixed cells were spotted onto the center of a 25.4 mm round silicon wafer support. Yeast control cells grown on normal media were used as a control for background levels of isotopes. The chip was then loaded into the NanoSIMS instrument and the electron multipliers were positioned to collect ^{12}C , ^{13}C , $^{12}\text{C}^{14}\text{N}^-$, and $^{12}\text{C}^{15}\text{N}^-$. The isotopic standard (yeast cells) was imaged first to calibrate the detector response before moving on to the test samples. Squares 20–30 μm in size were imaged until 80–100 cells had been imaged per test sample.

NanoSIMS image data were processed using the OpenMIMs plugin (<http://nano.bwh.harvard.edu/MIMSSoftware>) for ImageJ (<https://imagej.nih.gov/ij>). Hue/saturation/intensity (HSI) images were generated to visualize the isotope ratios for all samples. Regions of interest (ROIs) were then selected by defining each individual cell.

Agent-Based Simulation

Our simulation is based on the premise that microbial access to carbon and nitrogen resources can be modeled at the level of host macronutrient intake. We segregate the community of gut microbes into six ecologically distinct groups (guilds), each representing a unique strategy for acquiring their carbon and nitrogen, from distinct sources. Our modeling approach is summarized in Figure S6. A key feature of the model is that bacterial resource requirements are described in terms of just five sources: feed Prot, three types of feed Carb, and host proteoglycan (mucin).

We investigated microbial community responses to host nutritional intake by simulating the known intakes of 250 separately caged mice (Solon-Biet et al.,

2014), constituting 250 unique points in an intake landscape. These are represented in the Prot and Carb dimensions in Figure S6C. The mouse diet formulations were defined by systematically varying proportions of Fat, Prot, and Carb, and then diluting these with cellulose to modulate host-accessible nutrients. Prot comprised casein and methionine, and Carb comprised sucrose, wheatstarch, and dextrinized cornstarch. The simulation is parameterized on the basis that wheatstarch, dextrinized cornstarch, and sucrose represent digestion-resistant, partially resistant, and digestible Carbs, respectively. Although these designations are somewhat arbitrary, they allow us to investigate the effects of distinct Carb profiles on microbial community composition. Casein and methionine are grouped together in constituting simulated Prot. Beyond its diluting effect on intake of other macronutrients, Fat is mechanistically inert in our simulation, for not enough is known of its nutritional availability to microbes in the colon, and we have shown its influence on taxon-relative abundance responses to be marginal relative to Carb and Prot. Based on the observed daily average nutritional intakes of mice being unevenly split between night active (2/3) and day rest (1/3) (Jensen et al., 2013), 250 simulations were run for 3 weeks of simulated time, sufficient for the establishment of a stable microbial community (Figure 6B). At this point, the community composition for each of the 250 simulated mice is ascertained in terms of relative abundance of the six guilds (Figure S6D). Response landscapes describing each guild's change in relative abundance with nutritional intake are established by fitting generalized additive models to the data.

ACCESSION NUMBERS

Sequence data have been deposited to GenBank as a Metagenome Bio-project under the accession number GenBank: PRJNA257338.

SUPPLEMENTAL INFORMATION

Supplemental Information includes Supplemental Experimental Procedures, six figures, and two tables and can be found with this article online at <http://dx.doi.org/10.1016/j.cmet.2016.10.021>.

AUTHOR CONTRIBUTIONS

Microbiome Analyses, A.J.H., Y.V.C., F.C., J.B.C., and E.K.; Modeling, M.N.R. and A.J.H.; Animal Experiments and Phenotyping, S.M.S.-B., A.C.M., V.C.C., D.G.L.C., and S.J.S.; Statistical Analyses, K.R., A.J.H., and D.G.L.C.; Conceptualization and Funding Acquisition, D.G.L.C., D.R., and S.J.S.; Writing – Original Draft, A.J.H., S.J.S., and D.G.L.C.

ACKNOWLEDGMENTS

Funding was obtained from the Australian National Health and Medical Research Council (NHMRC project grant 571328), the Ageing and Alzheimers Research Fund of Concord RG Hospital, and the Sydney Medical School Foundation. Additionally, S.J.S. was supported by an Australian Research Council Laureate Fellowship; D.R. was partly funded by Gravida, the National Research Centre for Growth and Development, New Zealand; A.J.H. and Y.V.C. received a Travel and Access Program grant from the Australian Microscopy and Microanalysis Research Facility (AMMRF); and A.J.H. and E.K. were also supported by NHMRC project grant 1026209. We acknowledge the assistance of the Departments of Biochemistry and Anatomical Pathology, Concord RG Hospital. We thank Connie Ha, Timur Burykin, Szun Tay, and Patrick Bertolino for their contributions to other aspects of the study.

Received: July 1, 2016

Revised: August 30, 2016

Accepted: October 28, 2016

Published: November 23, 2016

REFERENCES

- Atarashi, K., Tanoue, T., Shima, T., Imaoka, A., Kuwahara, T., Momose, Y., Cheng, G., Yamasaki, S., Saito, T., Ohba, Y., et al. (2011). Induction of colonic regulatory T cells by indigenous Clostridium species. *Science* 331, 337–341.
- Berry, D., Stecher, B., Schintlmeister, A., Reichert, J., Brugiroux, S., Wild, B., Wanek, W., Richter, A., Rauch, I., Decker, T., et al. (2013). Host-compound foraging by intestinal microbiota revealed by single-cell stable isotope probing. *Proc. Natl. Acad. Sci. USA* 110, 4720–4725.
- Blondel, J. (2003). Guilds or functional groups: does it matter? *Oikos* 100, 223–231.
- Breuilard, C., Cynober, L., and Moinard, C. (2015). Citrulline and nitrogen homeostasis: an overview. *Amino Acids* 47, 685–691.
- Cani, P.D., Everard, A., and Duparc, T. (2013). Gut microbiota, enteroendocrine functions and metabolism. *Curr. Opin. Pharmacol.* 13, 935–940.
- Caporaso, J.G., Kuczynski, J., Stombaugh, J., Bittinger, K., Bushman, F.D., Costello, E.K., Fierer, N., Peña, A.G., Goodrich, J.K., Gordon, J.I., et al. (2010). QIIME allows analysis of high-throughput community sequencing data. *Nat. Methods* 7, 335–336.
- Claesson, M.J., Jeffery, I.B., Conde, S., Power, S.E., O'Connor, E.M., Cusack, S., Harris, H.M.B., Coakley, M., Lakshminarayanan, B., O'Sullivan, O., et al. (2012). Gut microbiota composition correlates with diet and health in the elderly. *Nature* 488, 178–184.
- Cotillard, A., Kennedy, S.P., Kong, L.C., Prifti, E., Pons, N., Le Chatelier, E., Almeida, M., Quinquis, B., Levenez, F., Galleron, N., et al.; ANR MicroObes consortium (2013). Dietary intervention impact on gut microbial gene richness. *Nature* 500, 585–588.
- Coyte, K.Z., Schluter, J., and Foster, K.R. (2015). The ecology of the microbiome: networks, competition, and stability. *Science* 350, 663–666.
- David, L.A., Maurice, C.F., Carmody, R.N., Gootenberg, D.B., Button, J.E., Wolfe, B.E., Ling, A.V., Devlin, A.S., Varma, Y., Fischbach, M.A., et al. (2014). Diet rapidly and reproducibly alters the human gut microbiome. *Nature* 505, 559–563.
- Derrien, M., Collado, M.C., Ben-Amor, K., Salminen, S., and de Vos, W.M. (2008). The Mucin degrader Akkermansia muciniphila is an abundant resident of the human intestinal tract. *Appl. Environ. Microbiol.* 74, 1646–1648.
- Devkota, S., Wang, Y., Musch, M.W., Leone, V., Fehlner-Peach, H., Nadimpalli, A., Antonopoulos, D.A., Jabri, B., and Chang, E.B. (2012). Dietary-fat-induced taurocholic acid promotes pathobiont expansion and colitis in IL10^{-/-} mice. *Nature* 487, 104–108.
- Donaldson, G.P., Lee, S.M., and Mazmanian, S.K. (2016). Gut biogeography of the bacterial microbiota. *Nat. Rev. Microbiol.* 14, 20–32.
- Donohoe, D.R., Garge, N., Zhang, X., Sun, W., O'Connell, T.M., Bunger, M.K., and Bultman, S.J. (2011). The microbiome and butyrate regulate energy metabolism and autophagy in the mammalian colon. *Cell Metab.* 13, 517–526.
- Faith, J.J., Guruge, J.L., Charbonneau, M., Subramanian, S., Seedorf, H., Goodman, A.L., Clemente, J.C., Knight, R., Heath, A.C., Leibler, R.L., et al. (2013). The long-term stability of the human gut microbiota. *Science* 341, 1237439.
- Faith, J.J., Ahern, P.P., Ridaura, V.K., Cheng, J., and Gordon, J.I. (2014). Identifying gut microbe-host phenotype relationships using combinatorial communities in gnotobiotic mice. *Sci. Transl. Med.* 6, 220ra11.
- Finucane, M.M., Sharpton, T.J., Laurent, T.J., and Pollard, K.S. (2014). A taxonomic signature of obesity in the microbiome? Getting to the guts of the matter. *PLoS ONE* 9, e84689.
- Jensen, T.L., Kiersgaard, M.K., Sørensen, D.B., and Mikkelsen, L.F. (2013). Fasting of mice: a review. *Lab. Anim.* 47, 225–240.
- Kashyap, P.C., Marcoval, A., Ursell, L.K., Larauche, M., Duboc, H., Earle, K.A., Sonnenburg, E.D., Ferreyra, J.A., Higginbottom, S.K., Million, M., et al. (2013). Complex interactions among diet, gastrointestinal transit, and gut microbiota in humanized mice. *Gastroenterology* 144, 967–977.
- Koropatkin, N.M., Cameron, E.A., and Martens, E.C. (2012). How glycan metabolism shapes the human gut microbiota. *Nat. Rev. Microbiol.* 10, 323–335.
- Lam, Y.Y., Ha, C.W.Y., Campbell, C.R., Mitchell, A.J., Dinudom, A., Oscarsson, J., Cook, D.I., Hunt, N.H., Caterson, I.D., Holmes, A.J., and Storlien, L.H. (2012). Increased gut permeability and microbiota change associate with mesenteric fat inflammation and metabolic dysfunction in diet-induced obese mice. *PLoS ONE* 7, e34233.

- Lam, Y.Y., Ha, C.W.Y., Hoffmann, J.M.A., Oscarsson, J., Dinudom, A., Mather, T.J., Cook, D.I., Hunt, N.H., Caterson, I.D., Holmes, A.J., and Storlien, L.H. (2015). Effects of dietary fat profile on gut permeability and microbiota and their relationships with metabolic changes in mice. *Obesity (Silver Spring)* 23, 1429–1439.
- Le Chatelier, E., Nielsen, T., Qin, J., Prifti, E., Hildebrand, F., Falony, G., Almeida, M., Arumugam, M., Batto, J.M., Kennedy, S., et al.; MetaHIT consortium (2013). Richness of human gut microbiome correlates with metabolic markers. *Nature* 500, 541–546.
- Le Couteur, D.G., Tay, S.S., Solon-Biet, S., Bertolino, P., McMahon, A.C., Cogger, V.C., Colakoglu, F., Warren, A., Holmes, A.J., Pichaud, N., et al. (2015). The influence of macronutrients on splanchnic and hepatic lymphocytes in aging mice. *J. Gerontol. A Biol. Sci. Med. Sci.* 70, 1499–1507.
- Lee, K.P., Simpson, S.J., Clissold, F.J., Brooks, R., Ballard, J.W.O., Taylor, P.W., Soran, N., and Raubenheimer, D. (2008). Lifespan and reproduction in *Drosophila*: new insights from nutritional geometry. *Proc. Natl. Acad. Sci. USA* 105, 2498–2503.
- Ley, R.E., Bäckhed, F., Turnbaugh, P., Lozupone, C.A., Knight, R.D., and Gordon, J.I. (2005). Obesity alters gut microbial ecology. *Proc. Natl. Acad. Sci. USA* 102, 11070–11075.
- Ley, R.E., Peterson, D.A., and Gordon, J.I. (2006a). Ecological and evolutionary forces shaping microbial diversity in the human intestine. *Cell* 124, 837–848.
- Ley, R.E., Turnbaugh, P.J., Klein, S., and Gordon, J.I. (2006b). Microbial ecology: human gut microbes associated with obesity. *Nature* 444, 1022–1023.
- Macfarlane, S., Woodmansey, E.J., and Macfarlane, G.T. (2005). Colonization of mucin by human intestinal bacteria and establishment of biofilm communities in a two-stage continuous culture system. *Appl. Environ. Microbiol.* 71, 7483–7492.
- Mattson, M.P., Allison, D.B., Fontana, L., Harvie, M., Longo, V.D., Malaisse, W.J., Mosley, M., Notterpek, L., Ravussin, E., Scheer, F.A., et al. (2014). Meal frequency and timing in health and disease. *Proc. Natl. Acad. Sci. USA* 111, 16647–16653.
- Mazmanian, S.K., Round, J.L., and Kasper, D.L. (2008). A microbial symbiosis factor prevents intestinal inflammatory disease. *Nature* 453, 620–625.
- Peters, J.H.C., Beishuizen, A., Keur, M.B., Dobrowski, L., Wierdsma, N.J., and van Bodegraven, A.A. (2011). Assessment of small bowel function in critical illness: potential role of citrulline metabolism. *J. Intensive Care Med.* 26, 105–110.
- Raubenheimer, D., and Simpson, S.J. (2016). Nutritional ecology and human health. *Annu. Rev. Nutr.* 36, 603–626.
- Ridaura, V.K., Faith, J.J., Rey, F.E., Cheng, J., Duncan, A.E., Kau, A.L., Griffin, N.W., Lombard, V., Henrissat, B., Bain, J.R., et al. (2013). Gut microbiota from twins discordant for obesity modulate metabolism in mice. *Science* 341, 1241214.
- Schloss, P.D., Westcott, S.L., Ryabin, T., Hall, J.R., Hartmann, M., Hollister, E.B., Lesniewski, R.A., Oakley, B.B., Parks, D.H., Robinson, C.J., et al. (2009). Introducing mothur: open-source, platform-independent, community-supported software for describing and comparing microbial communities. *Appl. Environ. Microbiol.* 75, 7537–7541.
- Simpson, S.J., and Raubenheimer, D. (2005). Obesity: the protein leverage hypothesis. *Obes. Rev.* 6, 133–142.
- Solon-Biet, S.M., McMahon, A.C., Ballard, J.W.O., Ruohonen, K., Wu, L.E., Cogger, V.C., Warren, A., Huang, X., Pichaud, N., Melvin, R.G., et al. (2014). The ratio of macronutrients, not caloric intake, dictates cardiometabolic health, aging, and longevity in ad libitum-fed mice. *Cell Metab.* 19, 418–430.
- Sonnenburg, E.D., and Sonnenburg, J.L. (2014). Starving our microbial self: the deleterious consequences of a diet deficient in microbiota-accessible carbohydrates. *Cell Metab.* 20, 779–786.
- Sonnenburg, E.D., Zheng, H., Joglekar, P., Higginbottom, S.K., Firbank, S.J., Bolam, D.N., and Sonnenburg, J.L. (2010). Specificity of polysaccharide use in intestinal *Bacteroides* species determines diet-induced microbiota alterations. *Cell* 141, 1241–1252.
- Sørensen, A., Mayntz, D., Simpson, S.J., and Raubenheimer, D. (2010). Dietary ratio of protein to carbohydrate induces plastic responses in the gastrointestinal tract of mice. *J. Comp. Physiol. B* 180, 259–266.
- Stecher, B., Robbiani, R., Walker, A.W., Westendorf, A.M., Barthel, M., Kremer, M., Chaffron, S., Macpherson, A.J., Buer, J., Parkhill, J., et al. (2007). *Salmonella enterica* serovar *typhimurium* exploits inflammation to compete with the intestinal microbiota. *PLoS Biol.* 5, 2177–2189.
- Wu, G.D., Chen, J., Hoffmann, C., Bittinger, K., Chen, Y.Y., Keilbaugh, S.A., Bewtra, M., Knights, D., Walters, W.A., Knight, R., et al. (2011). Linking long-term dietary patterns with gut microbial enterotypes. *Science* 334, 105–108.
- Wu, H., Tremaroli, V., and Bäckhed, F. (2015). Linking microbiota to human diseases: a systems biology perspective. *Trends Endocrinol. Metab.* 26, 758–770.
- Zhao, L. (2013). The gut microbiota and obesity: from correlation to causality. *Nat. Rev. Microbiol.* 11, 639–647.

Supplemental Information

**Diet-Microbiome Interactions
in Health Are Controlled by Intestinal
Nitrogen Source Constraints**

Andrew J. Holmes, Yi Vee Chew, Feyza Colakoglu, John B. Cliff, Eline Klaassens, Mark N. Read, Samantha M. Solon-Biet, Aisling C. McMahon, Victoria C. Cogger, Kari Ruohonen, David Raubenheimer, David G. Le Couteur, and Stephen J. Simpson

SUPPLEMENTAL FIGURES

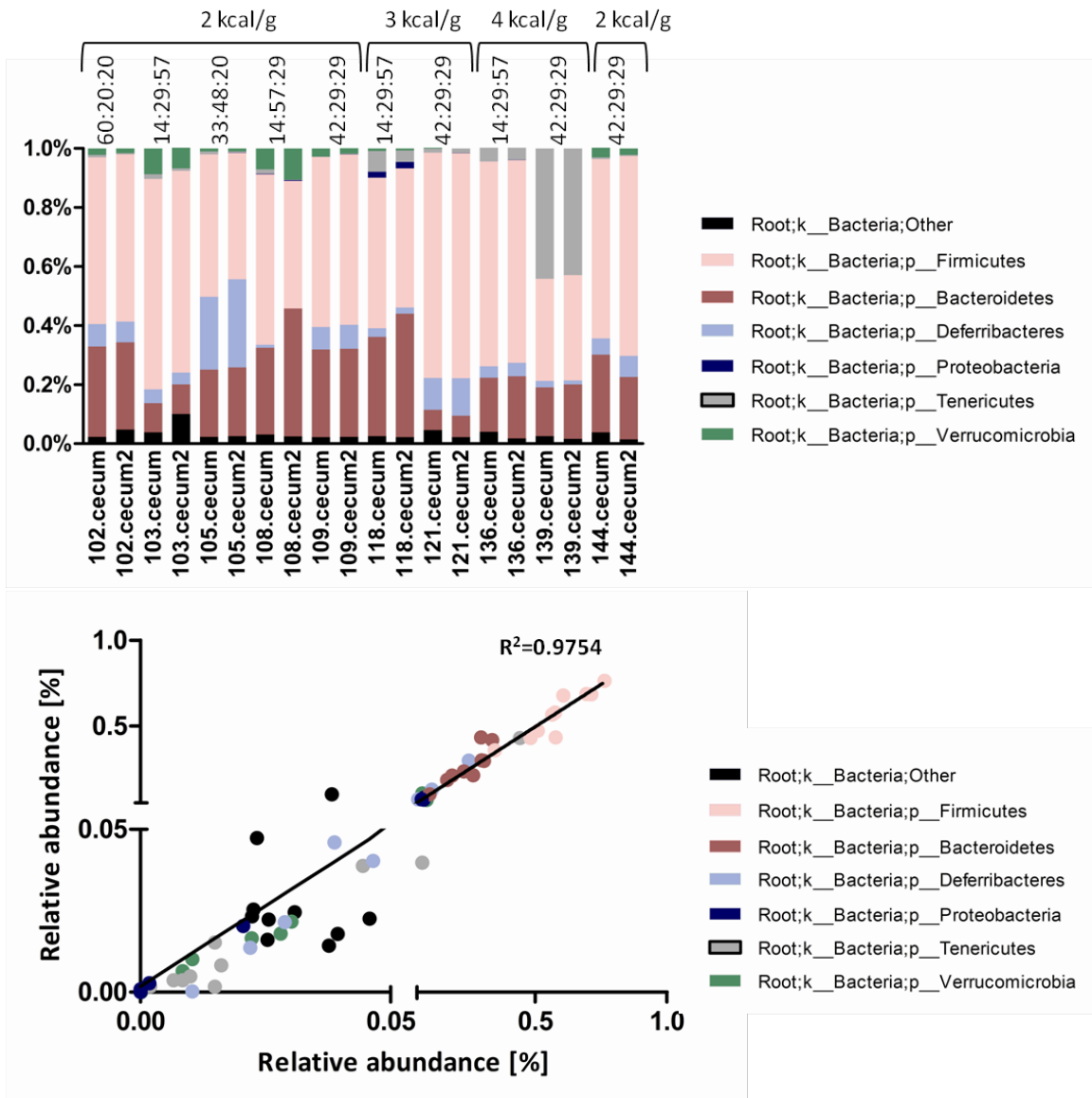


Figure S1, related to Figure 1A

Reproducibility of the sequence analysis was assessed by looking at 10 technical replicates from 5 different diets (60:20:20, 14:29:57, 33:48:20, 14:57:29 and 42:29:29) and 3 energy density regimes (2, 3 and 4 kcal/g). Independent processing commenced with independent DNA extraction from the same cecal suspension. Scatter plot shows replicates against each for the major higher taxa. Above 5% relative abundance reproducibility was extremely high. The poor correlation for Bacteria:Other almost certainly reflects imprecision associated with the classification between the replicates rather than the sequence generation.

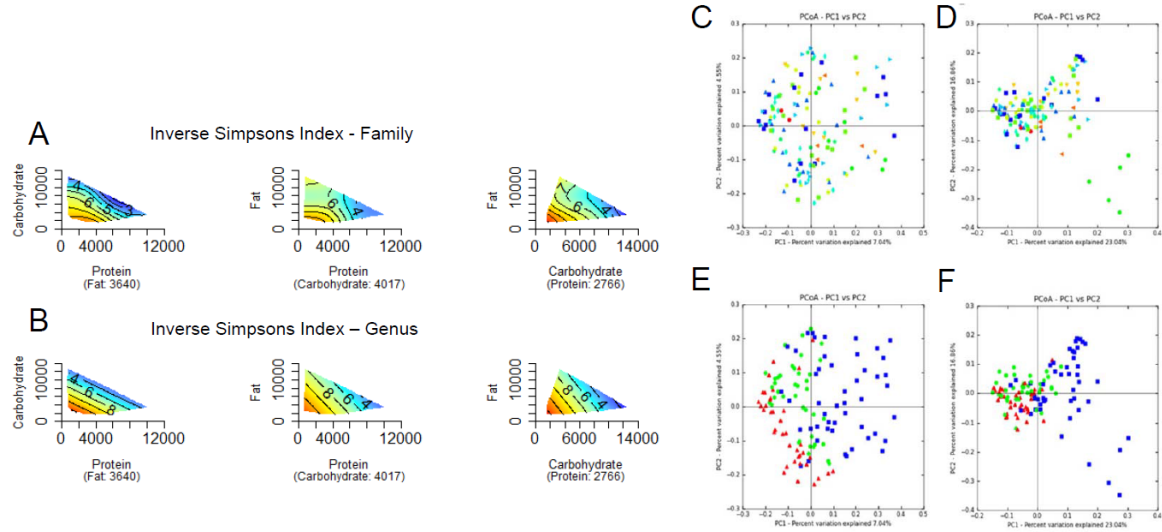


Figure S2, related to Figure 1B, C.

(A-B) Inverse Simpsons Index plotted against P, C and F intakes using the Geometric Framework method for microbiome family (A) and genus (B). Statistical significance is shown in Table S1.

(C-F) PCoA plots of Unweighted (C and E) and Weighted (D and F) UniFrac distances by diet treatment groups. Samples in panels C and D are coded by macronutrient distribution and in panels E and F by energy density (red 2 kcal, green 3 kcal, blue 4 kcal). The major effect is energy density but there is also separation within the 4 kcal diets by nutrient distribution. This is most obvious in the weighted analysis where the five animals on standard chow cluster separately (light green circles in panel D)

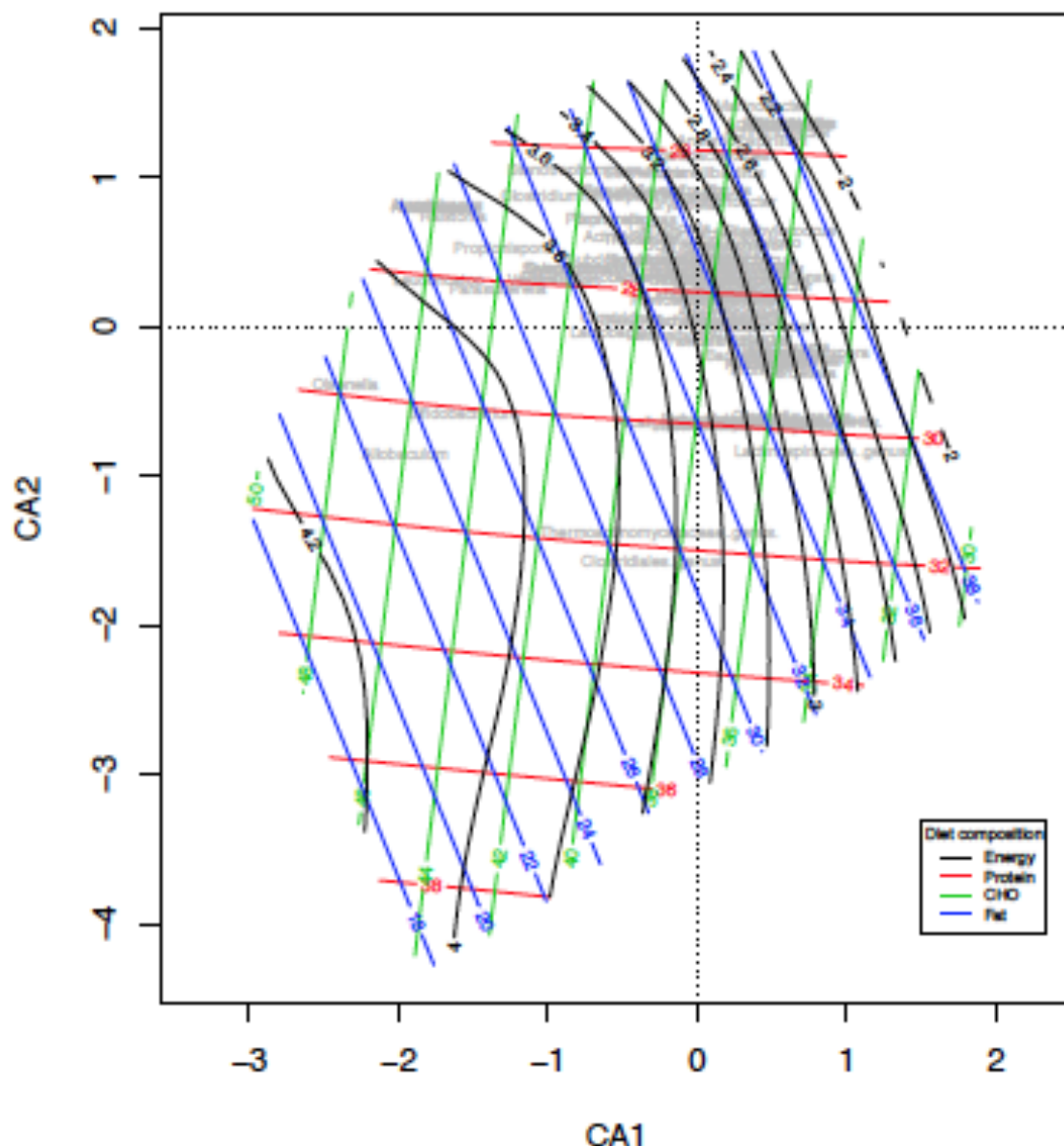


Fig. S3, related to Figures 1, 3

Unconstrained CA plot based on distribution of genera among the samples with the environmental gradients of diet composition fitted as a surface.

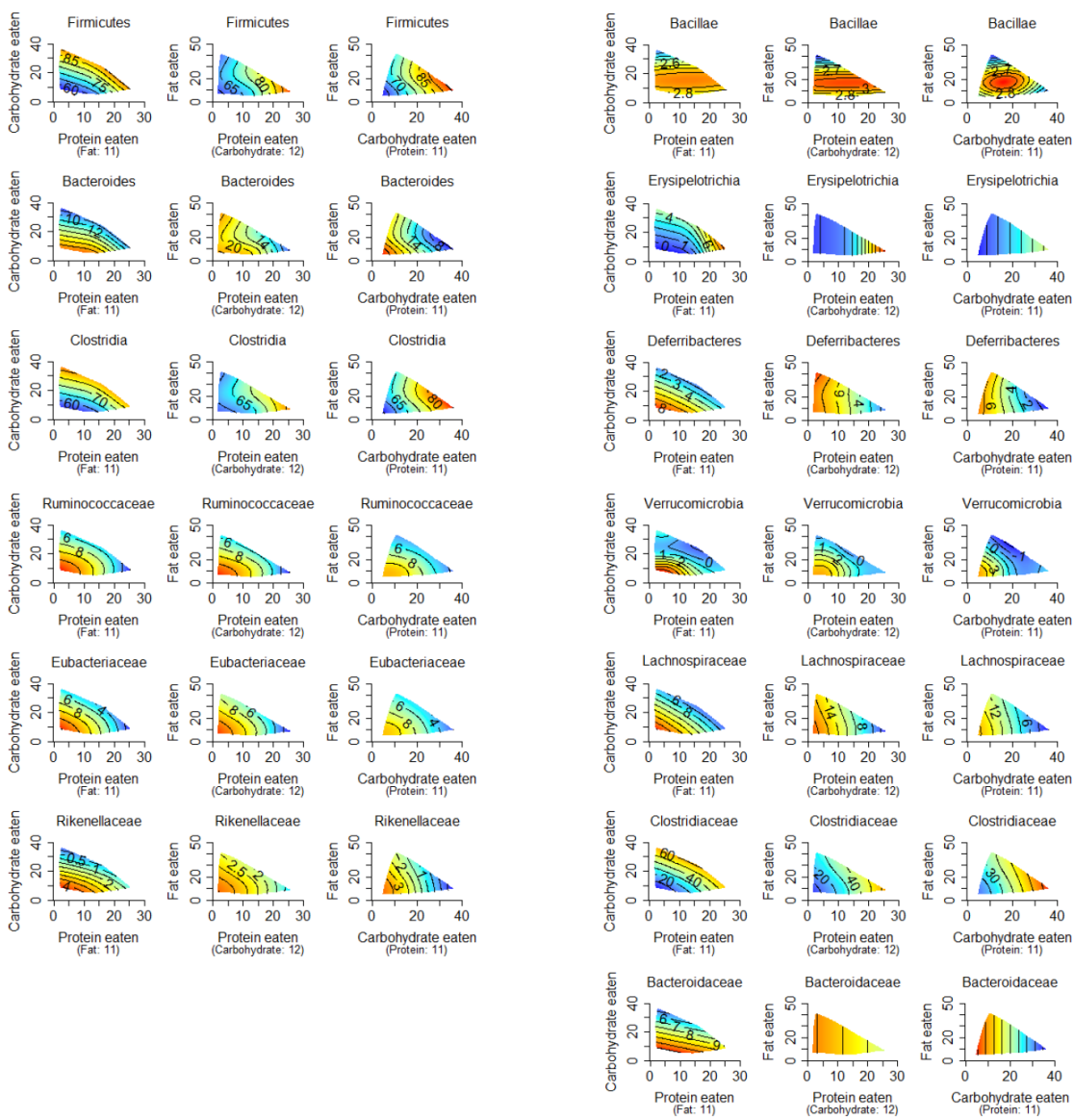


Figure S4 related to Figure 3.

Geometric Framework surfaces showing relationship between macronutrient intake and OTU abundance for all abundant OTUs from gut microbiota. For each OTU, surfaces are shown for the relationship between P, C and F intake versus relative abundance. The two-dimensional surface for each combination of two macronutrients is shown at the median of the third macronutrient. Red=highest abundance, Blue=lowest abundance. Statistical significance is shown in Table S1.

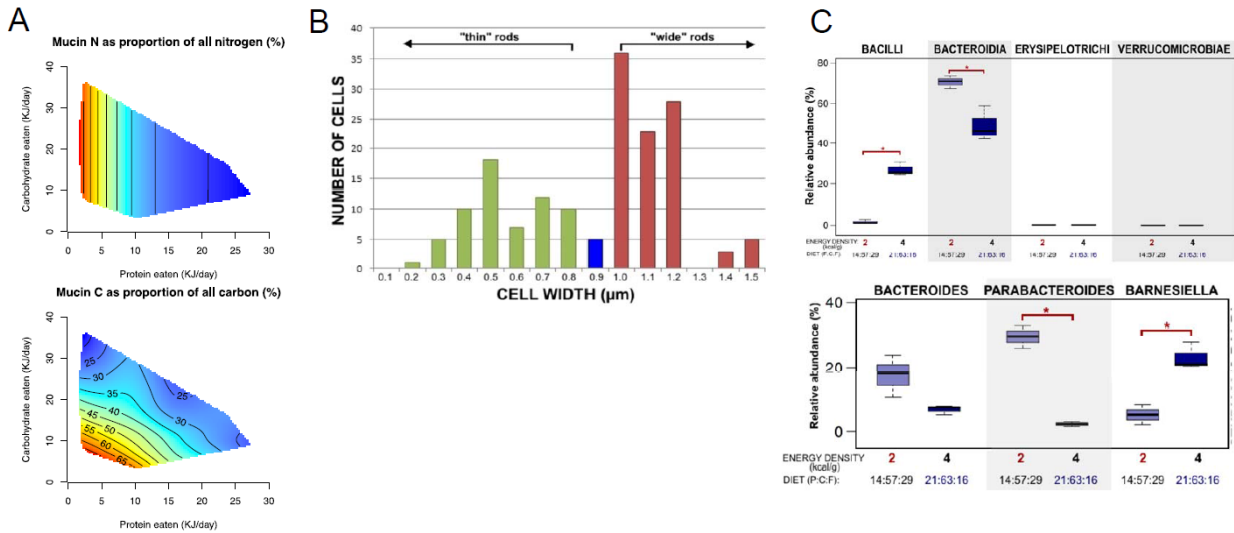
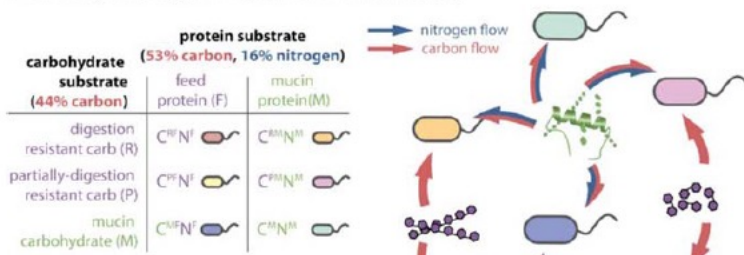


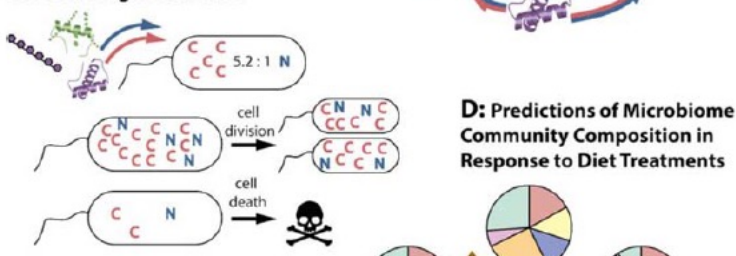
Figure S5 related to Figure 4.

- (A) Model simulations of mucin-derived carbon (Cm) or Nitrogen (Nm) available to bacteria as a proportion of total nutrient intake and macronutrients.
- (B) Bar chart showing frequency of cell widths observed in a representative set of 163 rod-shaped cells from mice on either a 4 kcal/g or 2 kcal/g energy density diet. Cells with width $\leq 0.8 \mu\text{m}$ were categorised as “thin” rods (green) while those with width $\geq 1.0 \mu\text{m}$ were classed as “wide” rods (red). Rods that were 0.9 μm in width were excluded from analysis as ambiguous.
- (C) Microbial diversity data from the threonine uptake experiment. A) Box-plots of relative abundances (%) of bacterial classes in samples from BALB/c mice on a standard diet (4 kcal/g energy density) or low energy density diet (2 kcal/g) with significance calculated using the Jaccard distance method. Diet-associated shifts in relative abundances of bacterial classes were observed with *Bacteroidia* and *Bacilli* responding significantly to changes in dietary energy intake. B) Box-plots of relative abundances (%) of genera within the *Bacteroidia* class in samples from BALB/c mice on a standard diet (4 kcal/g energy density) or low energy density diet (2 kcal/g) with significance calculated using the Jaccard distance method. Differential response to reduced host energy intake in groups within the class *Bacteroidia* were observed, with increase in relative abundances of *Bacteroides* and *Parabacteroides* and decrease in *Barnesiella* relative abundance.

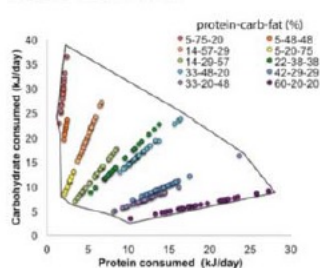
A: Conceptualizing the Gut Microbial Community



B: Modelling a Bacterium



C: Simulating a Range of Nutritional Intakes



D: Predictions of Microbiome Community Composition in Response to Diet Treatments

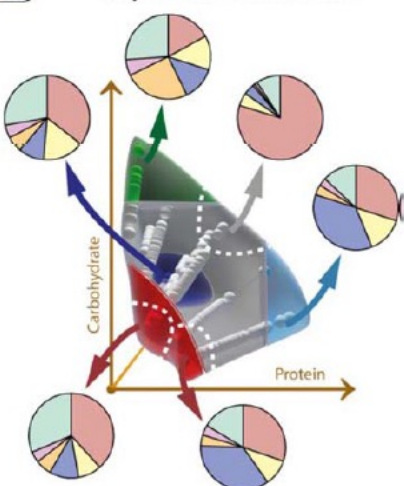


Figure S6 relating to Figure 5.

Predicting community composition of microbes characterized through nutrient acquisition strategy in response to diet treatment.

(A) The microbiome is conceptualized through microbe nutrient acquisition strategy, forming six trophic guilds. Each guild metabolizes a protein and carbohydrate substrate from which carbon and nitrogen, being the most readily limiting elements, are obtained. Both dietary and endogenous protein and carbohydrate sources are represented. We differentiate between digestion resistant and partially-digestion resistant dietary carbohydrate substrates. Guilds compete through overlapping substrate utilizations.

Guild colour indicators are maintained throughout all figures.

(B) The microbial community is simulated at the resolution of individual cells, which internalise carbon (C) and nitrogen (N) from their environment in accordance with guild membership. Internalised quantities of C and N decay with time, reflecting metabolic activity. Internalised C & N dictate a cell's fate: nutrient rich cells divide imminently, and starved cells die. A one-dimensional simulated gut environment harbours bacteria, and secretes mucin at constant rate uniformly along its length. Dietary nutrient is input at the

proximal end, following host-absorption; all fat and fully-digestible carbohydrates are absorbed, whereas digestion resistant and partially digestion resistant carbohydrates and dietary protein are absorbed at rates saturating with increasing dietary intake. Its load in relation to the gut carrying capacity determines the rate of bacteria and unutilized digesta defecation. Regular peristalsis events shuffle bacteria.

(C) 250 dietary intakes are independently simulated, defined by chow macronutrient distribution, energy density and average consumption of 250 cages of mice. Data are flattened along the fat axis. As fat is mechanistically inert in simulations, and protein & carbohydrate are primary drivers of community composition, subsequent figures show response landscapes plotted on protein & carbohydrate axes.

(D) The microbial community composition resulting from dietary treatment can be predicted. Community compositions following 3 weeks on a fixed diet are depicted; each composition is averaged from 10-17 simulations in the regions indicated.

SUPPLEMENTAL TABLES

Table S1 Summary of GAMS statistics. (Related to Table 1, Figure 3)

| | Consumption-type response (increase with intake) | | | | Limitation-type response (decrease with intake) | | | | Ecological relevance | | | |
|-------------------------------------|---|-----|---|----|--|-----|-----|-----|----------------------|-----|--------------------|--------|
| | P | C | F | PC | PCF | P | C | F | PC | PCF | Deviance explained | Scale |
| Total community metrics | | | | | | | | | | | | |
| Simpsons index (Family) | | | | | | *** | *** | * | | | 85.3% | 1.304 |
| Simpsons index (Genus) | | | | | | *** | *** | *** | | | 82.2% | 3.095 |
| Total abundance_Phylum level | | | | | | | | | | | | |
| Firmicutes | *** | *** | | | | | | | | | 30.3% | 160.2 |
| Bacteroidetes | | | | | | ** | *** | | | | 17.9% | 98.72 |
| Total abundance_Genus level | | | | | | | | | | | | |
| <i>Clostridium</i> | *** | *** | | * | | | | | | | 39.1% | 257.4 |
| Unnamed_Clostridiales | *** | *** | | | | | | | | | 36.7% | 34.31 |
| <i>Allobaculum</i> | . | | | * | | | | | | | 27.5% | 12.57 |
| <i>Lactobacillus</i> | . | | | | * | | | | | | 12.6% | 4.197 |
| <i>Bacteroides</i> | | | | | | * | | ** | | | 6.42% | 77.89 |
| <i>Eubacterium</i> | | | | | | *** | * | | | | 23.2% | 21.92 |
| <i>Akkermansia</i> | | | | | | ** | * | | * | ** | 31.3% | 11.69 |
| <i>Mucispirillum</i> | | | | | | ** | ** | | | | 12.3% | 40.94 |
| <i>Ruminococcus</i> | | | | | | *** | * | | * | | 19.8% | 15.65 |
| <i>Johnsonella</i> | | | | | | * | ** | | | | 7.17% | 6.7227 |
| <i>Alstipes</i> | | | | | | ** | *** | | | | 18.9% | 4.6567 |
| <i>Butyrivibrio</i> | | | | | | *** | | * | | | 20.5% | 2.0655 |
| <i>Parabacteroides</i> | | | | | | ** | | | | | 7.68% | 11.865 |
| <i>Blaelia</i> | | | | | | *** | | | ** | | 13.9% | 2.4658 |

Statistics for different community measures showing how significant responses are primarily seen for Protein and Carbohydrate intake. The ecological relevance of these statistics is influenced by the explained variation in the response surface and the relative strength of the measured parameter. For taxon abundance measures, the scale gives an indication of the relative proportion of the possible range of abundances that was captured in the model. Taxa whose relative abundance spans a wide range have a higher scale than those that were predominantly low abundance. Only the most abundant genera are shown. p<0.1; * p<0.05, ** p<0.01, ***p<0.001

Table S2, related to Figure 1

| Diet macronutrient distribution (Protein:Carb:Fat) | Energy density 2 kcal/g | Energy density 3 kcal/g | Energy density 4kcal/g |
|---|----------------------------|----------------------------|---------------------------|
| 60:20:20 | 6 mice 24.98 kJ/day | 5 mice 32.43 kJ/day | 4 mice 37.32 kJ/day |
| 42:29:29 | 6 mice 30.05 kJ/day | 5 mice 34.05 kJ/day | 3 mice 37.97 kJ/day |
| 33:48:20 | 3 mice 31.46 kJ/day | 6 mice 34.36 kJ/day | 5 mice 39.44 kJ/day |
| 33:20:48 | 5 mice 30.51 kJ/day | 6 mice 36.68 kJ/day | 5 mice 40.83 kJ/day |
| 23:38:38 | 5 mice 30.96 kJ/day | 5 mice 36.77 kJ/day | 3 mice 46.95 kJ/day |
| 14:57:29 | 3 mice 31.53 kJ/day | 5 mice 36.87 kJ/day | 6 mice 40.65 kJ/day |
| 14:29:57 | 4 mice 29.99 kJ/day | 3 mice 45.14 kJ/day | 5 mice 51.99 kJ/day |
| 5:75:20 | -- | 5 mice 37.49 kJ/day | 3 mice 40.47 kJ/day |
| 5:48:48 | -- | -- | 4 mice 46.27 kJ/day |
| 5:20:75 | -- | -- | 2 mice 54.03 kJ/day |

Diet treatment groups and average total energy intake for 112 mice in the 25 diet treatment groups. An additional 5 animals maintained on standard chow are not shown in this table. Two trends are evident, an increase in average energy intake per mouse with increased energy density of the diet (left to right) and increased average energy intake per mouse with decreasing proportion of protein in the diet (top to bottom).

Supplemental Experimental Procedures.

Long term nutrient intake experiment.

A total of 858 mice (strain C57Bl/6) were maintained on 25 diets of defined composition, and phenotyped at 15 months as described (Solon-Biet et al., 2014). Animals were recruited into the study in three cohorts and maintained on the diets *ad libitum* for their natural lifespan or until culling at 15 months. The diets comprised ten distinct macronutrient distributions supplied as protein (*casein and methionine*), carbohydrate (*wheat starch, dextrinised corn starch, and sucrose*) and fat (*soya bean oil*), each at up to 3 different caloric densities (Solon-Biet et al., 2014). The density of nutrients was determined by bulking out the food pellets with indigestible cellulose to create versions at 2, 3, and 4 kcal/g. All other ingredients were kept similar. Other ingredients include cellulose, a mineral mix (Ca, P, Mg, Na, C, K, S, Fe, Cu, I, Mn, Co, Zn, Mo, Se, Cd, Cr, Li, B, Ni and V) and a vitamin mix (vitamin A, D3, E, K, C, B1, B2, Niacin, B6, pantothenic acid, biotin, folic acid, inositol, B12 and choline) supplemented to the same levels as standard rodent chow AIN-93G (Specialty Foods, WA). Animals were housed in single sex groups of 3 per cage. Feed consumption was recorded per cage and transformed to estimate macronutrient and energy intake for individual animals (Table S2). Phenotype and amino acids were evaluated as described (Solon-Biet et al., 2014).

Microbial community analyses.

Bacterial community analyses were also conducted with fecal samples from BALB/c mice in the threonine tracer experiment. PCR for 16S rDNA and pyrosequencing were performed as described for the main data set. After initial processing, a total of 41 347 reads were obtained, ranging from 6 099 to 8 197 reads per sample. Trimmed and processed sequences were assigned to bacterial taxonomy using RDP Classifier, a hierarchical taxa assignment tool based on RDP naive Bayesian rRNA Classifier. A confidence threshold of 80% was used, where sequences below the threshold were designated as “unclassified”. The same general pattern for increased ratio of Bacteroidetes to Firmicutes on low energy density diet was seen, and again some within-phylum divergence of response was evident (Figure S5C). However, in this experiment with younger, BALB/c mice, Clostridiaceae were of much lower abundance and a much higher proportion of Bacteroidetes and Bacilli was seen. This highlights that although the absolute relative abundance values of Bacteroidetes and Firmicutes have limited predictive value across different host or diet systems, the factors driving their response appear to be similar.

High throughput sequence datasets are subject to both technical (reproducibility of sequence collection) and analytical (reproducibility of classification) variation. The resulting low level of precision means there is often inconsistency between diversity data from different studies and their relationship to ecological parameters. To address technical reproducibility, a subset of samples from the main study was independently processed twice to assess technical reproducibility (Fig S1). To account for the potential effects of ‘classification noise’ on identification of ecological drivers the data set was processed and classified by three different approaches and analyses were conducted at

multiple taxonomic scales. Although differences were seen in the relative abundance of several groups at the family or genus level within the Firmicutes and Bacteroidetes the general community composition was similar across classification approaches. Significantly, the associations between different aspects of nutrient intake or diet composition and directions of compositional change were consistent across all classification approaches. We conclude that the identification of ecological drivers of the microbial community is robust.

Diversity Assessment in relation to diet composition.

We first addressed the question; Does diversity differ between communities exposed to different diet compositions? The diversity of biological communities encompasses multiple dimensions, including species richness and evenness. Furthermore the scale of biological resolution (or evolutionary distance) for classification, and the sampling effort can also impact observations of diversity. To account for these variables, accumulation curves and diversity analyses were constructed at genus, family and class scale.

Across our data set the average reads per sample was 12,000 (Figure 1). When samples were combined into treatment groups defined by macronutrient composition (2-16 independent samples per treatment group) or energy density (32 - 40 samples per treatment group) accumulation curves show that at taxonomic scales above the rank of genus saturated sampling is predicted for each treatment group (Figure 2).

To explore which aspects of diversity were most sensitive to diet compositional variation we compared Rényi profiles for data sets clustered by energy density or nutrient distribution. The diversity series only showed significant separation between treatments for high values of α . This indicates that changes in evenness rather than species richness are the dominant response. Comparisons of analyses clustered by nutrient distribution or by energy density further showed that energy density is the dominant diet composition factor for alpha diversity when viewed at genus or family scale. At the class scale there was no significant difference observed for separations by energy density or for most nutrient distributions (data not shown).

Beta diversity, or compositional differences between the diet treatment groups were examined using ordinations of datasets based on both correspondence and principal coordinates analyses. The main text shows an unweighted unifrac PCoA plot with the by energy density treatment for each sample labelled (Figure 1C). Here for comparison we also show this ordination labelled by macronutrient profile and similar paired representation for the weighted unifrac PCoA plots (Figure S2C-F). In both ordinations separation of the samples from 4 kcal/g treatments is seen separations based on macronutrient distribution are much less well-defined. In the weighted unifrac analysis the % variation explained is higher.

To further resolve the effects driving differences in the communities we also explored the relationship between environmental gradients and community composition using correspondence analyses based on the taxonomic categorizations. Again, there is a strong

separation of the two lowest energy samples (2 and 3 kcal/g) from the majority of the high energy density (4 kcal/g) samples. In Figure S3 the gradient surface is fitted on the basis of the samples' locations in diet space and the taxon locations can be interpreted as the maximum occurrence in relation to the fitted environmental gradients of diet composition. The surface fitting is with generalised additive models (GAM) using thin-plate splines. Despite many gradient variables having a p-value below 0.01 the fits were greatest in explanatory power for energy density (62.4%) and to a lesser extent fat (11.0%). Therefore, it may be concluded that the ordination of the samples more strongly follows the dietary treatments of energy density and fat than other parameters.

Taxon responses in relation to nutrient intake.

Owing to animal digestive and absorptive processes, not all ingested food is available to microbes. Furthermore, this will vary with the composition of the food and the intake pattern. This is an especially important consideration for *ad libitum* feeding studies, since animals self-regulate food intake to reach nutritional targets.

These considerations mean that several factors with potential to influence competition for nutrients between members of the microbial community in the gut will vary interdependently across the diet treatment groups. These include total dry matter and energy intakes, total amount of each macronutrient eaten (as Protein, Carbohydrate or Fat), and the ratio of macronutrients ingested. Accordingly, we have used nutritional geometry to disentangle these factors. Explanatory power was greatest for taxa that were frequently represented at levels greater than 1% relative abundance across the 25 diet treatment groups. Finer-scale taxa (individual OTUs) were generally of lower abundance and are not shown here. However their response surfaces typically corresponded to one of the described response guilds as presented for the higher taxa in the main text.

Modelling intestinal nitrogen availability.

For microbial ecosystems, limiting nutrients are typically described in terms of sources of major bioelements such as carbon and nitrogen. To explore the relative availability of mucin nutrient sources to the microbial ecosystem, we constructed a simple model. The model assumes that dietary protein, are carbohydrate are both sources of Carbon, but that the only sources of Nitrogen are dietary protein and mucin. The model also assumes that the host extracts a proportion of dietary C and N before food reaches the colon. Across the range of modelled host extraction proportions (50-70% for Carbon and 65-95% for Nitrogen) the models of the relative availability of mucin-derived to diet-derived Nitrogen and Carbon show a broad increase in relative availability of mucin-derived nitrogen on low energy density diets (Figure S5). This is consistent with ability to access mucin-derived N (and to a lesser extent C) having the potential to provide competitive advantage to Bacteria under low nutrient intake conditions.

Model simulation.

Gutsim is an agent-based model of gut bacterial community dynamics described in terms of guild composition. The framework for this model and further interpretation of the simulations are described below. A Python implementation of the model is available on request.

Our simulation is based on the premise that microbial access to carbon and nitrogen resources can be modeled at the level of host macronutrient intake. It is well established that carbohydrate sources vary in the extent to which they resist digestion and absorption in the small intestine to become microbially available (Flint *et al.* 2008; Rogowski *et al.* 2015). Thus microbially available carbon will be sensitive to dietary carbohydrate profile. Although protein is also a carbon source, our data indicate that the major impact of protein intake is via nitrogen availability. We predict microbially available nitrogen will be relatively insensitive to dietary protein profile since excess absorbed nitrogen still becomes available to microbes through excretion into the small intestine (Kawasaki *et al.* 2015).

Figure S6 summarises our modelling approach. We use computational simulation to test the following:

- 1) That the ability to monitor dynamics using the guild-based approach is similar to phylogenetic-based approaches of comparable taxonomic granularity;
- 2) That simulated manipulations of response drivers for guilds generate similar patterns to those observed for real taxa assigned to the guilds in experimental manipulation;
- 3) That the dominant nutritional selection pressure for community members will vary according to both microbe-dependent (life history strategy) and diet-dependent (food composition and intake) effects.

Conceptualising the microbial community.

We segregate the community of gut microbes into six ecologically distinct groups (*guilds*), each representing a unique strategy for acquiring their carbon (C) and nitrogen (N), from distinct sources (Figure S6A). This is comparable resolution to bacterial phyla (gut communities are typically dominated by just 6-10 types). The python implementation of these guilds is defined towards the end of the module `gutsim/bacteria.py` (supplementary materials). To explore the community dynamics resulting from this abstraction a number of operational assumptions were applied with regard to other aspects of the host-microbiome system. First is the assumption that all bacteria in a guild will respond similarly to a host's nutritional intake, regardless of other aspects of within-guild diversity. For each guild, members utilize one carbohydrate source and one protein source to obtain carbon (C) and nitrogen (N). All other essential elements (e.g. P, S, O, H) are assumed to be available in non-limiting quantities. We consider both diet- and host-derived substrates, and spatio-temporal dynamics to model microbial fate, occupation and transit through the gastro-intestinal tract (GIT). We consider the total host intake to constitute fat, protein and carbohydrates with microbial access to these to further influenced by host processes. We simplify the carbohydrate profile as comprising digestible, digestion-resistant and partially-digestion resistant carbohydrates. Digestible carbohydrates and fat are unavailable to microbes (assumed to be entirely absorbed by the host). Dietary protein, digestion resistant and partially resistant carbohydrates; together with the glycan and protein components of mucin, form substrates available to colonic microbes. Pairwise combinations of these two proteins and three carbohydrates defines six guilds, which compete through their overlapping substrate utilization. Through these abstractions of colonic nutrient availability we can investigate

how the balance of C and N flow from either endogenous or exogenous sources shapes the microbial community.

Diet-derived microbial growth substrates include digestion resistant and partially digestion resistant carbohydrates, and protein. Host-derived microbial growth substrates include the glycan and protein components of mucin.

Modelling a bacterial cell's state.

Our simulation is agent-based, and we represent each individual bacterium as a unique and explicit entity inhabiting a specific location in the simulated GIT space (Figure S6B). A bacterial cell acquires C and N by internalising substrates from its environment in accordance with its guild's nutrient acquisition strategy. A cell's fate is determined by its quantities of internalised C and N. Cellular function requires a ratio of 5.2C:1N be maintained (Vrede *et al.* 2002), excess of either element beyond this ratio confers no benefit. Hence, either C or N status can limit the function and viability of each individual cell (Figure 6B). A cell will not internalise additional quantities of the non-limiting nutrient. As a cell's internalised quantity of C & N increases, so too does its probability of division. Conversely, cells that are relatively nutrient starved face a higher probability of death. Death and division rates as a function of limiting nutrient are implemented at the top of the module bacteria.py (supplementary materials).

Representation of the gut environment.

We have estimated the proportion of daily nutrient intake that the host absorbs (Silvester *et al.* 1995), which asymptotically approaches a saturating maximum quantity as daily intake increases. Non-host-sequestered nutrient is available to microbes. Microbe locations in the simulated gut determine the substrate profiles they have access to, the profiles resulting from nutrient input and the history of microbial activity. Dietary nutrients enter at the proximal end, and both unused substrate and bacteria are excreted at the terminal end. Mucin secretion rates have been estimated from literature (MacFarlane *et al.* 2005; Bansil *et al.* 2006; Ermund *et al.* 2013). Mucin is secreted at a constant rate, evenly spread along the length of the gut. Secretion rate does not change with diet, a necessary assumption in absence of more information. Peristalsis waves shuffle bacteria and nutrients as they traverse the gut (Roberts *et al.* 2007). An upper limit on the gut's microbe carrying capacity has been estimated, and if exceeded is enforced by increasing the defecation rate. The different aspects of the nutrient supply and gut motility dynamics are implemented in the modules experiment.py (mucin secretion rate), feed-regimen.py (temporal dynamics of all components) and mouse.py/Mouse.execute (spatial distribution of bacteria and nutrients in colon).

Supplemental References

Bansil R., and Turner B.S. (2006) Mucin structure, aggregation, physiological functions and biomedical applications. *Curr. Opin. Colloid Interface Sci.* *11*, 164-170.

Ermund A., Gustafsson J.K., Hansson G.C, and Keita A.V. (2013) mucus properties and goblet cell quantification in mouse, rat and human ileal Peyer's patches. *PLoS One* *8*, 83688Flint H.J., Bayer E.A., Rincon M.T., Lamed R.A., and White B.A. (2008) Polysaccharide utilization by gut bacteria: potential for new insights from genomic analysis. *Nature Rev. Microbiol.* *6*, 121-131.

Kawasaki K., Min X., Li X., Hasegawa E., and Sakaguchi E. (2015) Transfer of blood urea nitrogen to cecal microbial nitrogen is increased by fructo-oligosaccharide feeding in guinea pigs. *Animal Sci. J.* *86*, 77-82.

Rogowski A., Briggs J.A., Mortimer J.C., Tryfona T., Terrapon N., Lowe E.C., Basle A., Morland C., Day A.M., Zheng H. et al. (2015) Glycan complexity dictates microbial resource allocation in the large intestine. *Nature Comm.* *6*, 7481.

Silvester K.R., Englyst H.N, and Cummings J.H. (1995) Ileal recovery of starch from whole diets containing resistant starch measured in-vitro and fermentation of ileal effluent. *Am. J. Clin. Nutr.* *62*, 403-411.

Vrede K., Heldal M., Norland S., and Bratbak G. (2002) Elemental composition (C, N, P) and cell volume of exponentially growing and nutrient-limited bacterioplankton. *Appl. Environ. Microbiol.* *68*, 2965-2971.